NOVA SCHOOL OF SCIENCE & TECHNOLOGY

DEPARTAMENT OF MATERIALS SCIENCE

Filipa da Cruz Fonseca de Matos

BSc in Micro and Nanotechnology Engineering

Nature-derived Conductive Substrates for Therapeutic Applications

MASTER IN Micro and Nanotechnology Engineering

NOVA University Lisbon

September, 2023

DEPARTAMENT OF
MATERIALS SCIENCE

NOVA SCHOOL OF
SCIENCE & TECHNOLOGY

Nature-derived Conductive Substrates for Therapeutic Applications

Filipa da Cruz Fonseca de Matos

Master/BSc in Micro and Nanotechnology Engineering

Adviser: Doctor Henrique Vazão de Almeida,
Researcher, FCT-NOVA

Examination Committee:

Chair: Doctor Maria Helena Figueiredo Godinho,
Associate Professor, FCT-NOVA

Rapporteur: Doctor Paula Isabel Pereira Soares,
Principal Researcher, FCT-NOVA

Adviser: Doctor Henrique Vazão de Almeida,
Researcher, FCT-NOVA

MASTER IN MICRO AND NANOTECHNOLOGY ENGINEERING

NOVA University Lisbon
September 2023

Nature-derived Conductive Substrates for Therapeutic Applications

This document was created with Microsoft Word text processor and the NOVA thesis Word template.

ACKNOWLEDGEMENTS

Firstly, I would like to acknowledge Prof. Dr. Elvira Fortunato and Prof. Dr. Rodrigo Martins for providing access to the Micro and Nanotechnology Engineering course which gave me the knowledge and the opportunity to grow throughout these five years.

I would like to thank my coordinator Henrique Almeida for the advice, motivation, support and help during the whole project, as well as all the opportunities he gave me, not only to learn more, but also to be part of such an innovative project.

Then I would like to thank all the guidance and support provided by FCT NOVA and CENIMAT's collaborators during the time I was working in the laboratory, and for the opportunity to use high-quality equipment and materials. A special thanks to Maria Morais, Tomás Pinheiro, and Claúdia Pereira who accompanied and helped accomplish all the procedures done during this project.

I also want to thank José Inácio for the availability to guide me through the cell culture experiments, and for the opportunity to work with cardiac cells.

Finally, I want to thank Jules Guillaud for his excellent work during the time he was with us, and for being so helpful. Additionality, I would like to thank my work colleagues Margarida Barata, Catarina Lourenço, Carolina Jorge, and Mariana Oliveira for the time we spent together in the laboratories helping each other and sharing live experiences.

ABSTRACT

This thesis investigates the potential of polysaccharide-based conductive substrates, integrated with laser-induced graphene (LIG), as a novel platform for cardiomyocyte culture with the future prospect of utilizing it for cardiomyocyte (CM) maturation through electrical stimulation techniques.

The methodology involves the fabrication of LIG within different polysaccharide-based matrices, including chitosan, agarose, and alginate, through a single step laser process using a low-cost infrared (CO_2) laser. Comprehensive characterization of these composite substrates is conducted, encompassing electrical conductivity, mechanical and chemical properties, and biocompatibility tests. Subsequently, human induced pluripotent stem cell-derived cardiomyocytes (hiPSC-CMs) culture experiments are carried out to assess the substrate's effectiveness in supporting cardiomyocyte metabolism, morphology, and functionality.

Findings reveal that the LIG produced in polysaccharide films showed sharp characteristic Raman peaks and reasonable sheet resistance values. Besides, the LIG-polysaccharide substrates offered an appropriate conductive environment ($\approx 2\ S.m$) for cardiomyocyte culture, promoting cell attachment, viability, and metabolic activity. This research signifies a significant step towards a sustainable and biocompatible substrate for cardiac tissue engineering. Additionally, the study explores the potential for employing electrical stimulation techniques to enhance cardiomyocyte maturation on these substrates.

The implications of this research are profound, as it conciliates sustainable biomaterials and cardiac tissue engineering, offering a promising avenue for developing functional cardiac tissue constructs and advanced strategies for cardiac regenerative therapies. In conclusion, this work contributes to the evolving landscape of cardiac tissue engineering and underscores the potential of LIG-polysaccharide substrates as a versatile platform for both cardiomyocyte culture and future maturation techniques through electrical stimulation.

Keywords: human induced pluripotent stem cell-derived cardiomyocytes (hiPSC-CMs), laser induce graphene (LIG), polysaccharide materials, sustainability, biocompatibility.

RESUMO

Este trabalho tem como principal objetivo avaliar o potencial de substratos condutores à base de polissacarídeos, integrado com grafeno induzido por laser (LIG), como uma plataforma inovadora para a cultura de cardiomiócitos, com a perspetiva futura de utilizá-los para a maturação de cardiomiócitos por meio de técnicas de estimulação elétrica.

A metodologia usada envolve a fabricação de LIG em diferentes filmes de polissacarídeos, nomeadamente de quitosano, agarose e alginato, através da incidência de um laser infravermelho (CO_2) de baixo custo. É feita uma caracterização detalhada dos substratos, analisando a condutividade elétrica, propriedades mecânicas e químicas, e testes de biocompatibilidade. Posteriormente, é realizada cultura de cardiomiócitos derivados de células-tronco pluripotentes induzidas humanas (hiPSC-CMs) para avaliar a eficácia do substrato em promover o crescimento, morfologia e funcionalidade dos cardiomiócitos.

Os resultados revelam que os substratos de LIG-polissacarídeo oferecem condutividade adequada para a cultura de cardiomiócitos $\approx 2\ S.m$, promovendo a sua adesão, viabilidade e metabolismo. Esta pesquisa representa um passo significativo para a engenharia de tecido cardíaco, uma vez que comprova a fabricação de substratos sustentáveis e biocompatíveis. Além disso, o estudo explora o potencial dos substratos em técnicas de estimulação elétrica para aprimorar a maturação de cardiomiócitos.

Os desenvolvimentos desta pesquisa são úteis, pois explora o uso de biomateriais sustentáveis em engenharia de tecido cardíaco, oferecendo uma direção promissora para o desenvolvimento de tecido cardíaco funcional e estratégias avançadas para terapias regenerativas cardíacas. Em conclusão, este trabalho contribui para a evolução da engenharia de tecido cardíaco e destaca o potencial dos substratos de LIG-polissacarídeo como uma plataforma versátil tanto para a cultura de cardiomiócitos como para futuras técnicas de maturação por estimulação elétrica.

Palavras-chave: Cardiomiócitos derivados de células-tronco pluripotentes induzidas humanas (hiPSC-CMs), grafeno induzido por laser (LIG), materiais polissacáridos, sustentáveis, biocompatíveis.

CONTENTS

LIST OF FIGURES

LIST OF TABLES

NOTATION

W_w	Weight of wet film
W_d	Weight of dry film
W_f	Weight of fully dried film
t_{LIG}	LIG thickness
R_{Sheet}	Sheet Resistance
ρ	Resistivity
σ	Electrical Conductivity

1. CONTEXT AND MOTIVATION

Cardiovascular diseases are the leading cause of mortality worldwide, killing over seventeen million people each year, and heart failure is one of the most common risk factors [1]. The adult human heart has an extremely low capacity to regenerate, with a cardiomyocyte (CM) renewal rate estimated at 1% a year, which decreases with age [2]. CMs are the cardiac cells, responsible for the involuntary and rhythmic contractions of the heart, providing the necessary pump action through the circulatory system [3]. Heart failure is caused by the loss of CMs, so it is crucial to have regenerative therapies focused not only on maintaining the remaining CMs but also, on regenerating and maturing lost ones [4]. The immaturity of CMs regenerated by the currently used strategies, such as Pluripotent Stem Cells (PSC), has become their major limitation as the use of these cells is restricted, especially for pharmacological and therapeutic purposes [5]. Here we aim to develop innovative matrices for future use in maturation of CMs, using sustainable and low-cost approaches. For this, we studied the use of polysaccharide-based biopolymers functionalized with laser-induced graphene (LIG), as platforms for hiPSC-CMs culture.

1.1 Introduction

Tissue engineering (TE) seeks to produce specific human tissues, by combining specific cell types and extracellular scaffolds [6]. The major difficulty is to have an artificial scaffold that mimics the extracellular matrix (ECM), to guarantee cell adhesion, migration, differentiation, and proliferation *in vitro* and *in vivo* [6]. Porosity, topography, surface functionalization, mechanical and electrical properties, biocompatibility, biodegradation, and non-toxicity are essential features to evaluate when selecting materials for TE applications [6].

1.1.1 Biomaterials for Cardiac Tissue Engineering

Biomaterials, in particular, polymeric biomaterials have been commonly used in cardiac tissue engineering, due to their tunable properties, and the possibility of functionalizing or adding other materials to enhance their performance [6]. Both synthetic and natural polymeric biomaterials have been thoroughly studied and used for cardiac tissue engineering. Regarding synthetic polymers, polyethylene glycol (PEG) , poly L-lactide (PLLA), DL-glycolide-co-lactide (PLGA), and poly caprolactone (PCL) are widely used for these applications, however, these materials present some concerns regarding their synthesis processes which can be complex, expensive, not sustainable, and present possible toxicity [6], [7]. Within the natural polymers family, the use of collagen [8], gelatin [9], fibrin [10], silk fibroin [11], alginate [12], cellulose [13], and chitosan [14] has been reported in several studies as promising

materials for biomedical applications. Besides their high biocompatibility, natural biopolymers induce a very weak inflammatory response *in vivo*, and are a favorable environment for cell viability. Although their attractive advantages, natural biopolymers are known for their weak mechanical properties, and fast degradation kinetics, which can affect their performance in TE [15]. For use in CTE, is important to that the artificial scaffold mimic the myocardium tissue environment, for that it must present properties such as mechanical, chemical and thermal stability, flexibility, and electrical conductivity. Natural biopolymers are divided into two main types: polysaccharides, such as chitosan and alginate, and proteins, such as collagen and gelatin [7]. Polysaccharides have been considered promising materials for TE, especially due to their high biocompatibility, good availability, and tailorable properties. Polysaccharides are characterized by having long carbohydrate molecules of monosaccharide units joined together by glycosidic bonds [16]. These materials have been widely applied for the regeneration of almost all tissues, such as myocardium, bone, cartilage, skin, liver, skeletal muscle, and neural tissue, as well as for the encapsulation and delivery of biological molecules [16]. These biopolymers can be used in the form of injectable hydrogels, porous and fibrous scaffolds, films, or membranes [16]. To improve the performance of biopolymers for TE, the combination of the beneficial biological properties of natural polymers with the excellent mechanical performances of synthetic ones, has been thoroughly investigated [15].

1.1.2 Electrical Stimulation for Cardiac Tissue Engineering

Electrical stimulation of cells is commonly used to induce coordinated contraction of cardiac tissues and for the maturation of several cell types. For instance, it has been proved that this stimulation has an impact on the rate, duration, and the number of action potentials in CMs, which consequently affect the amount of beating cells, their synchronization and calcium handling in the CMs network [17]. Many studies are already focusing on the electrical stimulation of CMs, proving its potential in CM gene nd protein expression [17]. Electrical stimulation can be achieved using a simple setup with two electrodes that apply electrical fields directly to the cell culture media. The electrodes used can be made of carbon or platinum and the optimization of the electrical parameters is essential to manipulate cell response in the biomaterial system [17]. Researchers have been putting a lot of effort into improving cell culture platforms to efficiently align and mature CMs. The addition of conductive materials, such as graphene, to the cell substrate or matrix to improve the conduction between CMs, is a strategy used to improve the efficiency of this approach [18]–[20].

1.1.3 Graphene

Graphene is a two-dimensional (2D) hexagonal matrix, like a honeycomb structure, and it is present in nature in the form of graphite, which has multiple layers of graphene held by Van der Walls forces [21]. The graphene family, containing pristine graphene (pG), graphene oxide (GO), and reduced graphene oxide (rGO), have shown a strong potential for therapeutic applications, due to their unique properties, especially their high conductivity, biocompatibility, and excellent electromechanical properties [21], [22]. Although its promising properties, standard graphene production has some weaknesses, such as high costs, non-sustainability, complexity, and possible cytotoxicity [21], [23].

1.1.4 Laser-Induced Graphene (LIG)

Recently, laser-induced graphene (LIG) appeared as an alternative to standard graphene production, as it allows a fast and cost-effective synthesis of graphene, which was initiated by converting polyimide into a graphene foam, upon exposure to a CO_2 infrared laser [24], [25]. This process consists in a laser that emits photons upon a carbonaceous substrate, modifying their surface into aromatic structures, that resemble the graphene structure [21]. It is an excellent alternative to conventional graphene with tunable morphology, porosity, and composition. Additionality, this approach allows the simultaneous patterning and production of LIG decreasing the overall time of the process. Besides that, LIG uses scalable and roll-to-roll compatible methods, is sustainable, flexible, robust, and has excellent electrical and thermal properties, essential features for TE applications [24]. Tour and co-workers have demonstrated laser-fabricated graphene on lignin-containing, cellulose-based biomaterials (cork, potato skins, coconut shells) by multiple lasing using a CO_2 laser [26].

Depending on the application, the correct laser choice, appropriate threshold power, and laser speed are essential features to form high-quality LIG. The presence of carbons in the sp^2 hybridized aromatic content of the precursor material has also shown great improvement in this technique [21]. The fabricated graphene by laser scribing is not a sheet of 2D material but a 3D structure, that can have multiple layers of graphene with random orientations and can have different forms, such as flakes, fibers and foam [21]. This means that these graphitic structures are independently flexible and strong at the micro-scale, while on a macro-scale, they show a very fragile and brittle behavior [21]. The characterization of these features, by sheet resistance measurements, and Raman spectroscopy, is crucial to evaluate and compare the effect of different laser operation parameters and the properties of the graphitic materials produced from laser irradiation [27]. Recently, innovative studies have demonstrated that organic materials can be directly modified into conductive graphitic carbon by laser irradiation, paving a new way in this technique [21], [28], [29].

This progress has opened a new way in the bioelectronics industry as it will allow the fabrication of electronic devices in biomaterials, guaranteeing their sustainability and non-toxicity [23]. Laser graphitization on natural biopolymers can also be promising for TE, as LIG, can be used to improve their electrical conductivity, enhancing their performance in studies with cells *in vitro* and *in vivo*.

1.2 Strategy

This work is focused on the use and testing of three polysaccharide biopolymers, from marine sources, namely chitosan, alginate, and agarose, as a conductive matrix for cardiac cell experiments *in vitro* as a proof of concept to exhibit their viability for future application in the electrical stimulation of cells, **Figure 1**.

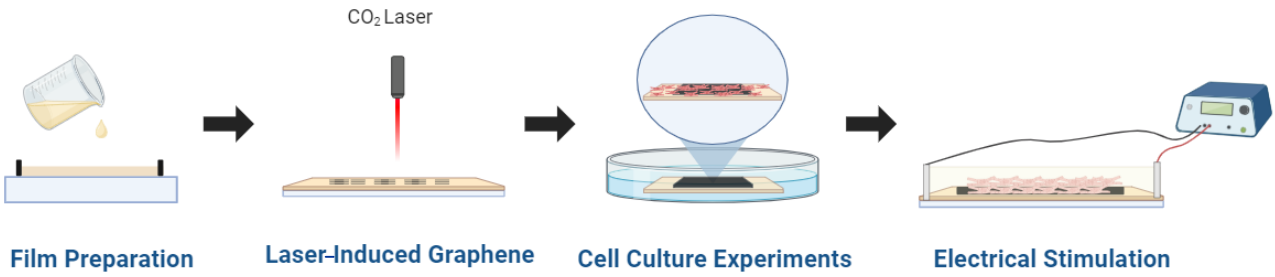

Figure 1. Schematic of the strategy used in this work, representing the main steps: film preparation, laser-induced graphene, cell culture experiments and electrical stimulation of cells. Created in BioRender.com.

Chitosan (CS), one of the most abundant polysaccharides, is derived from chitin's deacetylation and is composed of randomly distributed deacetylated units, β-(1→4)-linked D-glucosamine, and acetylated units, N-acetyl-D-glucosamine. Chitosan has been widely used in biomedical applications, due to its biocompatibility, biodegradability, non-toxicity, and high affinity towards biological molecules [14], [30]. Unlike chitin, chitosan is soluble in aqueous acetic acid and in most common polymer solvents, which facilitates its usage. Besides, it has acidic pH electrolyte properties, cationic nature, and possesses reactive functional groups, which make it suitable for different applications in various forms, such as gels, hydrogels, films, membranes, and nanoparticles. Although the use of pure chitosan as scaffolds for TE has limitations, such as poor mechanical stability and a high degradation rate, this can be overcome by combining chitosan with synthetic materials [6].

Alginate (AL) is an anionic and hydrophilic polysaccharide, composed of blocks of (1–4)-linked β-D-mannuronic acid (M) and α-L-guluronic acid (G) monomers. It has been used as a supporting matrix and delivery system for tissue regeneration, especially as an injectable hydrogel [12], [16]. Being a natural polysaccharide, alginate exhibits a pH-dependent anionic nature and can interact with cationic polyelectrolytes. As chitosan, alginate molecular weight (MW) influences the degradation rate and

mechanical properties of alginate-based biomaterials, thus it is crucial to select the right MW when using as a scaffold for TE [12]. It is biocompatible, biodegradable, it is soluble in postmodified salts and has tunable viscosity. However, alginate has inadequate mechanical stability for TE, so composite scaffolds are preferred by combining alginate with other materials or use additional crosslinking methods [6].

Agarose (AG) is a linear polymer consisting of repeating monomeric units of agarobiose (a disaccharide of D-galactose and 3,6-anhydro-lgalactopyranose) [16]. It has excellent biocompatibility, thermo-reversible gelation behavior and physiochemical properties [31]. It is a versatile material as it can be used as construct, hydrogels, and 3D-printed scaffolds. Agarose is a suitable medium for cell encapsulation due to its high-water uptake capability, and maintenance of spherical cell morphology [31]. It is usually combined with other polymers and proteins to improve its mechanical and electrical properties [31].

For the three polysaccharides, the combination with other polymers and materials is crucial to ensure stability and improve their performance, not only in the production of LIG but also in cell culture experiments. In this study three different modifications will be tested: I) the addition of lignin, II) the addition of fire retardant (sodium tetraborate) and III) the addition of both lignin and sodium tetraborate to improve the conversion of the substrates into LIG.

Lignin is an abundant amorphous natural polymer, found in the cell wall of plants, and an inexpensive by-product of paper industry. Besides, lignin molecular structure contains aromatic content, which makes it an effective precursor material for LIG [21], [32], [33]. Miyakoshi's group proved that the concentration of lignin added to the agarose hydrogel affected the crystallite size, conductivity, and dimensions of the fabricated graphitic structure [28]. However, lignin is a relatively insoluble material and can contain toxic impurities, which makes it difficult for cells to attach and grow on its surface. In Melanie L. Hart's study, it was proved that low molecular weight (MW) lignin at adequate concentration does not show cytotoxicity in *in vitro* studies with human cell types [34]. So, it is important to carefully choose lignin type and concentration when using lignin for TE applications. The addition of a fire retardant to biopolymers is essential for laser scribing once it can reduce their flammability or prolong their rate of survivability when exposed to high temperatures [35]. Sodium tetraborate (borax) is frequently used as a crosslinking agent for several polymers, such as chitosan, acting as an intermolecular bond reinforcer, and introducing covalent bonds that reinforce the natural hydrogen bonding [36]. Additionality, as its decomposition process is endothermic, it helps to protect the substrate' structure. Besides, borax can act as a protective barrier against bacteria and fungi due to its antimicrobial and fungicidal properties [36]. According to European Food Safety Authority (EFSA), sodium tetraborate does not raise concerns for genotoxicity [37]. The modifications of the natural biopolymers will allow the improvement of the mechanical properties of the substrates, the production of high-efficiency LIG, and

consequently enhance their mechanical and electrical performance as a matrix for experiments with cells.

2. MATERIALS AND METHODS

This section describes the materials and protocols used during the development of the polysaccharide conductive substrates for cell experiments *in vitro*. It is divided into three main parts: the production and characterization of biopolymer films followed by the laser scribing process and LIG characterization. Finally, cell culture experiments performed in this work are detailed.

2.1 Film Preparation

Reagents and chemicals: Chitosan (low molecular weight), sodium alginate, agarose, acetic acid (99-100% purity), glycerol, sodium tetraborate (decahydrate), lignin (alkali) were purchased from Sigma-Aldrich and used without further purification. Distilled water was used throughout the experiments. In this section, 3 film groups were produced with similar formulations: 3.75 to 5 % (w/v) of polysaccharide material, 1.5 to 2 % of glycerol, and 0.375 to 0.5 % (w/v) of lignin or/and borax.

Chitosan-based films Preparation: Chitosan film was obtained by dissolving 0.75 g of chitosan powder in 15 ml of acetic acid solution 5% (v/v), making a 5% (w/v) chitosan concentration. Then 0.3 ml of glycerol was added, as a plasticizer. The obtained solution was heated at 80 °C in a stirring plate for 1 h, to homogenize components and then sonicated for 1 h to remove trapped air bubbles. Finally, the sonicated solution was cast on glass and air-dried at room temperature for several days [29]. For the chitosan/borax, chitosan/lignin and chitosan/borax/lignin a 15 ml of 5 % (v/v) acetic acid solution was prepared and then borax powder or/and lignin powder were added separately and left to stir for 24 h. Then, 0.75 g of chitosan and 0.3 ml of glycerol were slowly added to the solution while stirred, heated up at 80 ºC for 1 hour and left stirring overnight at room temperature, to dissolve all the components. Four films were produced in this section: chitosan, chitosan/borax, chitosan/lignin, and chitosan/lignin/borax.

Agarose-based films Preparation: Agarose-only film was produced by dissolving 0.3 ml of glycerol in 15 ml of distilled water by stirring and heating the solution at 110 ºC until complete dissolution. Then 0.75 g of agarose powder was added to the solution and stirred for 30 min. Agarose/borax solution was prepared by dissolving 0.075 g of borax powder in 15 ml of distilled water with glycerol and stirring for 2 hours. Then agarose was added, and the solution was heated at 110 ºC and stirred for about 2 hours. For agarose/lignin and agarose/borax/lignin solutions a 5% (v/v) acetic acid solution with 0.5 % of lignin was prepared previously. Then the right amount of glycerol and borax powder were slowly added to the acidic solution, separately. After stirring for 2 hours, agarose was added while stirring and heated at 110 ºC until all components were fully dissolved. Immediately before the solvent casting step, the solutions were placed in a conventional microwave for a few seconds, to ensure that

the agarose solution was liquid. Four films were produced in this section: agarose only, agarose/borax, agarose/lignin, and agarose /lignin/borax.

Alginate-based films Preparation: Alginate films were produced similarly to agarose ones, but with slight differences in the concentrations, due to solubility concerns: 3.75 % (w/v) alginate, 1.5 % (v/v) glycerol, 0.375 % (w/v) borax and 0.375 % (w/v) lignin. The procedure was similar to agarose films preparation. The alginate film was done by dissolving first the right amount of glycerol in 20 ml of distilled water, and then the alginate powder was added while stirring at room temperature. As the solution became very viscous, the temperature was heated up at 110 ºC for 2 h to dissolve all the components. Alginate/borax solution was prepared by dissolving borax powder in the 20 ml distilled water with glycerol solution. Then the alginate was added, and the solution was stirred at 110 ºC for 2 h. For agarose/lignin and agarose/borax/lignin solutions a 5% (v/v) acetic acid solution with 0.5 % of lignin was prepared previously. Then the right amount of glycerol and borax powder were slowly added to the acidic solution, separately. After stirring for 1 hour, alginate was added while stirring and heated at 110 ºC until all chemicals were fully dissolved. Immediately before the solvent casting step, the solutions were placed in the microwave for a few seconds, to ensure that the solution was liquid. Four films were produced in this section: alginate only, alginate/borax, alginate/lignin, and alginate/lignin/borax. When fully dried, a crosslinking method was performed to avoid the dissolution of alginate when in solution. The four alginate films were submersed in a 100 mM $CaCl_2$ solution with 10 mM HEPES for 10 min and air dried until fully dry.

For the 3 groups, the solvent casting of the films was done by pouring the final solutions into a 10×10 cm glass, with a mold made with tape, making a rectangular shape of 8.5 × 4 cm for each film and let air dry at room temperature for a few days (See appendix **A1 Figure 16**). Twelve flexible films were produced in this section, with similar thicknesses and areas. All films were stored with a constant humidity and temperature, until fully dried.

2.1.1 Film Formulations

This section summarizes the films produced in this work, which will be discussed and analyzed in the following sections. The samples are divided into three main groups, based on the main material used: G1: chitosan films, G2: agarose films, and G3: alginate films. The conformation of each film is illustrated in appendix **A2 Figure 17**.

Table 1. Composition of produced polysaccharide films, with the different modifications with borax and lignin.

	G1: Chitosan films
A	5% CS+2% GC
B	5% CS+2% GC+0.5% B
C	5% CS+2% GC+0.5% LG
D	5% CS+2% GC+0.5% B+0.5% LG
	G2: Agarose films
E	5% AG+2% GC
F	5% AG+2% GC+0.5% B
G	5% AG+2% GC+0.5% LG
H	5% AG+2% GC+0.5% B+0.5% LG

	G3: Alginate films
I	3.75% AL+1.5% GC
J	3.75% AL+1.5% GC+3.75% B
K	3.75% AL+1.5% GC+3.75% LG
L	3.75% AL+1.5% GC+3.75% B+3.75% LG

*CS: chitosan, AG: agarose, AL: alginate; GC: glycerol, B: borax, LG: lignin.

2.1.2 Films Characterization

This section describes the analysis done to evaluate the physical and mechanical properties of the produced films. For that, film thickness, swelling degree, and degradation ratio are analyzed.

Thickness: The thickness of the dry films was measured using a digital micrometer (Mitutoyo, resolution 1 μm) by reading accurately at different points within the films and averaging it.

Swelling and degradation tests: The evaluation of the stability of films was done by swelling degree ratio and degradation ratio in a phosphate buffered saline (PBS) solution (pH=7.4), to understand their behavior in a cell culture medium for different periods of time. The swelling test was done in all films without graphitization, to evaluate the mechanical properties of the polysaccharide materials. The degradation test was performed only with the 3 chosen groups to be used in cell culture, which were the ones that presented Raman spectroscopy and sheet resistance of LIG. For all the samples, a droplet of 0.5 % gelatin solution was fixed into the LIG and let it dry at room temperature. The main objective was to guarantee that the graphitic structure maintained attached to the film while immersed in the cell culture medium, to assure its electrical properties during all the experiments.

Swelling Degree, % (SD): Swelling studies were performed by cutting 1 × 1 cm squares (n = 3 per group and per time point) of the dried biopolymer films prepared previously and weighting them (Wd). Afterwards, the samples were submersed in PBS solution (pH=7.4) at room temperature for 48 hours. At different periods of time (10min, 30min, 1h30min, 3h, 24h, and 48h) the films were taken out of the PBS solution, gently wiped with paper to remove surface moisture, and then weighed again (Ww) [14]. The swelling degree was calculated according to equation (1), where Ww is the weight of the wet film and Wd is the weight of the dry film.

$$Swelling\ Degree\ (\%) = \frac{Ww - Wd}{Wd} \times 100 \quad (1)$$

Degradation Ratio (Weight Loss (%)): Degradation studies were performed by cutting 1 × 1 cm squares (n = 3 per group and per time point) of the film with visible graphitization and adding a droplet of 5 % gelatin solution into it. The dried samples were weighted before the experiment (Wd). Afterwards, the samples were incubated in PBS solution (pH=7.4) at 37 ºC for different periods of time (1 day, 5 days, 7 days, and 14 days). Following each immersion, the samples were carefully removed from the medium and weighed after drying at 40°C until fully dried (Wf) [14]. The weight loss was calculated based on the mass loss using equation (2).

$$Weight\ Loss\ (\%) = \frac{Wd - Wf}{Wd} \times 100 \quad (2)$$

2.2 Laser Graphitization

Graphitic structures were fabricated using a VLS3.50 Universal laser system, consisting of a CO_2 laser with 10.6 μm wavelength, and 50 W of maximum power and scanning speed of 1.27 m/s (raster mode). Square patterns, designed in Adobe Illustrator software, were fabricated by raster scanning of the laser beam to create the graphitic pattern on the surface of fully dried biopolymers. Laser power (P), speed (S), and focal distance (Z) were optimized for each film, according to their thickness. The distance between the nozzle of the laser and the surface of each film was fixed at the value 0.327''. Thus, each film has specific values for P, S and Z parameters. For the 3 groups of films, only one laser scanning step was needed to achieve visible graphitization.

LIG production: For all films, laser parameters were tested and optimized by doing a matrix of 2 × 2 mm squares with different laser power, to evaluate its influence on the properties of the produced graphitic structures (See appendix **A3 Figure 18**). Then the LIG was analyzed to investigate its performance, by studying its morphological, chemical, and electrical properties.

2.2.1 LIG Characterization

The morphological, chemical, and electrical properties of LIG were analyzed for each film. Firstly, SEM was used to assess the morphology and thickness of the graphitic material to calculate its resistivity. Afterwards, Raman Spectroscopy was made to evaluate the presence of graphitic material, and then sheet resistance measurements were made to ensure the conductivity of the functionalized films.

Scanning Electron Microscopy (SEM): The morphological study was done by SEM, with both TM3030Plus and Regulus SU8220 Hitachi, with Au/Pd coating (20 nm), for the evaluation of LIG thickness, porosity, and surface roughness. With this study it is possible to see the modification of film

topography upon laser scribing, and the different porous graphitic materials produced in the different films. For this cross-section and top view samples of each sample were analyzed and measured using Image J software.

Raman Spectroscopy: Raman spectroscopy analysis was performed using a Reninshaw Qontor Raman Microscope equipped with a 532 nm laser and a 600 l/mm grating. For all samples 3 different areas were analyzed.

Electrical Conductivity: The electrical conductivity of the LIG produced in the different films was evaluated through a high-performance Hall Effect Measurement System, with a high-impedance buffer amplifier (HL5500PC). For these measurements, LIG samples were cut from the different films, and contacts were done by depositing droplets of Ag ink in the corners of the 4 × 4 mm squares. If the thickness of LIG is known it is possible to calculate its bulk resistivity (Ω.m) through equation (3), where Rsheet is the sheet resistance (Ω/sq) and t is the LIG thickness.

$$\rho = R_{sheet} \times t_{LIG} \quad (3)$$

Electrical conductivity (σ) was then calculated as the inverse of the resistivity (ρ):

$$\sigma = 1/\rho \quad (4)$$

2.3 Cell Culture Experiments

The cell culture experiments were done by producing LIG squares of 7 × 7 mm in each film, followed by the deposition of 0.5 % (v/v) gelatin solution to ensure the consistency of LIG during all the experiments. Besides, all samples were sterilized before any experiment.

Sterilization of the sample: The sterilization of samples was done by a 20 min bath in a 70 % ethanol solution, inside a laminar flow hood with ultraviolet light (UV) light.

Differentiation of hiPSCs into Human Cardiomyocytes: The cell culture was performed using undifferentiated single hiPSCs which were expanded in Essential 8 Medium in a 12-well plate. Differentiation started by replacing the medium from each well with 1.5 ml of RPMI supplemented with B27 serum without Insulin (GibcoTM), supplemented with 12 μM CHIR, 100ng/ml Activin A, and 270 μM of Ascorbic Acid, to induce CM differentiation. The procedure done along the culture period followed a previously published protocol [38].

Live/Dead staining: The viability of the cells in contact with the samples and their morphological changes were assessed on day 0 (8 hours), 3, and 5. For this test 80:20 ratio of cell culture medium and gelatin, respectively, was used. The images were captured using a Carl Zeiss Axiovert 40 inverted microscope and analyzed using ImageJ software [39].

Presto Blue Assay: The cell proliferation in the film samples was tested with the Presto Blue (Invitrogen) assay at four different time points; day 0 (8 hours), 3, and 5. The assay was carried out according to the manufacturer's protocol [39]**.**

Scanning Electron Microscopy (SEM): Cells cultured on the LIG produced on the biopolymers were fixed with 4% paraformaldehyde (PFA) for 15 min and then washed 3 times with PBS. The samples were dehydrated through baths of 5 min in 50%, 70%, 80, 90%, and 100% ethanol solutions, respectively, at room temperature.

Immunofluorescence staining: The immunofluorescence staining was done after fixation as described above. Firstly, the permeabilization of the samples with PBS and 0.1% Triton X was done, followed by blocking with 2% BSA (bovine serum albumin) solution, 30 min each. Then the samples were incubated with primary antibody (Monoclonal Anti-α-Actinin) in the blocking solution (1:800) and washed 3 times with PBS. The incubation with secondary antibody (Goat anti-Mouse IgC) was done also in blocking solution (1:500) for 1 hour, followed by a wash in PBS. Finally, the samples were stained with DAPI in PBS for 15 min and washed 3 times.

Statistics: Results are expressed as mean ± SD, with n = 3 per group and time point. Single factor analysis of variance (ANOVA) was used to determine statistical significance within a data set. If ANOVA detected a significant difference within the data set, Tukey HSD post-hoc test was used to determine significant differences between groups. Differences were significant when $p < 0.05$.

3. RESULTS AND DISCUSSION

This chapter presents the results and discussion of procedures done to study the topology of the prepared films, and the efficiency of LIG production. The results of performed cell culture tests are also presented. The three different groups of films, G1, G2, and G3, whose compositions are described in section 2.1.1, were analyzed to evaluate the best formulations for their performance as matrix for cell culture experiments.

3.1 Film Characterization

Physical and mechanical properties of the films, specifically the thickness, and swelling degree were assessed, to evaluate their viability for further analysis.

3.1.1 Thickness

The results, **Table 2**, showed that chitosan-based films (G1), were the thinner ones, while agarose-based films (G2), films were the thickest. The alginate-based films (G3) presented variable values of thickness, this was expected as during the drying process these films became folded and wrinkled.

Table 2. Thickness measurements of all films, using a digital micrometer (±1 µm).

G1	Thickness (µm)	G2	Thickness (µm)	G3	Thickness (µm)
CS	181 ± 18	**AG**	361 ± 34	**AL**	192 ± 56
CS+B	127 ± 3	**AG+B**	368 ± 95	**AL+B**	281 ± 136
CS+L	216 ± 14	**AG+L**	248 ± 110	**AL+L**	161 ± 14
CS+B+L	190 ± 3	**AG+B+L**	287 ± 50	**AL+B+L**	288 ± 45

Results are expressed as mean ± SD (n=3).

3.1.2 Swelling degree

The capability to swell after absorbing liquid is an important property to evaluate in films used for cell cultures experiments, since it influences the nutrient and metabolite infiltration, and, consequently, the cell behavior. The swelling ability of biopolymers is dependent on various factors, such as thickness, drying process, thermodynamic compatibility, polymer relaxation time, interaction with the functional groups of the biopolymer, and crosslinker chain structure and chemical properties [40]. Biopolymers, such as polysaccharides, have some drawbacks related to their mechanical properties, presenting poor mechanical stability in water, due to their hydrophilic nature. This analysis showed the swelling behavior in PBS solution of the different films produced for different time periods, with results presented in **Figure 2**.

Firstly, the SD values of the different films showed significant variation, ranging from 5% to 800%, approximately. There were different results between the three polysaccharide groups, showing the different behavior of the materials when in solution. The high values of SD may be influenced by the drying method of the films used in this work, solvent casting, because this process allows for extended chain conformation which leads to the exposure of hydrophilic functional groups of the biopolymers to the surface [41]. Additionally, the presence of a plasticizer, glycerol, can influence the water sensitivity of polysaccharide films, as it forms hydrogen bonding with water molecules. So the presence of glycerol in the film's formulation, increase the water affinity and thus, lead to higher moisture content, solubility, water vapor permeability and elongation at break of these films [42]. Besides this, the water uptake by biopolymers has already been proved to may be reversely dependent on the thickness, being higher for thinner films. This finding can be explained as thinner films present higher surface area, and consequently higher interaction between the water molecules and biopolymer molecules [43].

The results presented in **Figure 2 a)** show that chitosan-based films have the highest swelling degree values, confirming the inverse relationship between the film's thickness and absorption ability, as chitosan-based films were the thinner films produced. Films where only borax was incorporated in their formulation (CSB, AGB, and ALB) showed an increase in the SD compared with the films without modification. This can be explained as borax forms hydrogen bonding with water leading to a higher absorption ability [44]. On the contrary, the incorporation of lignin into polysaccharide films may lead to a decrease in water molecules adhesion, since lignin molecules will interact with the free hydrophilic groups via hydrogen bonds, making a hydrophobic interaction. **Figure 2** shows that, for the three groups, films with lignin in their formulation present lower swelling degree, proving the influence of lignin in water absorption. For cell culture experiments it is essential to guarantee a high-water resistance of films, for long periods of time, thus lignin addition showed to be an important additive to assure the film's mechanical stability during all the experiments [45]. Besides, although borax led to a high swelling degree, its presence helps to improve mechanical and solubility resistance, as well as thermal conductivity of films, once it acts as an intermolecular bond reinforcer, introducing covalent bonds [36]. So, the films that have both borax and lignin in their formulation may have lower water absorption, as there are less free bonds where water molecules can interact. In **Figure 2,** it is possible to confirm that CSBL, AGBL, and ALBL samples have lower swelling degree then the other films formations within the same group. For cell culture experiments, moderately swelling matrices are preferred as they form a porous surface, acting as an anchor for the cells, improving cell adhesion [40]. In the appendix (**A4 Figure 19)** is presented the swelling degree curve for all samples in different periods of time.

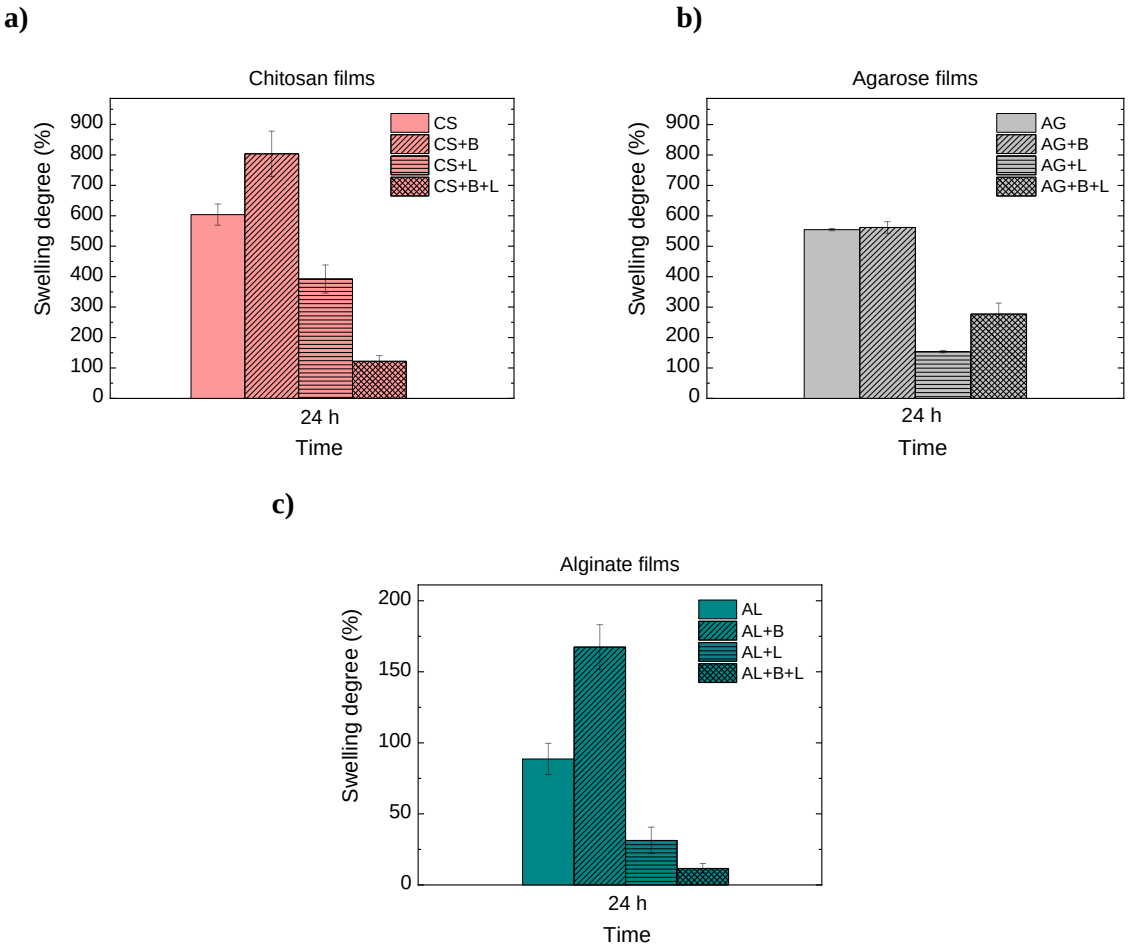

Figure 2. Swelling Degree data of the different film formulations after 24 h immersion in PBS solution (pH 7.4, RT). **a)** chitosan films, **b)** agarose films, **c)** alginate films. Data are shown as % increase in the film weight, as means ± SD (n=3). p value > 0.05 indicating no significant differences between groups.

3.2 LIG Fabrication

The synthesis of LIG on the different substrates was carried out by testing various combinations of laser parameters, namely power (P), scan speed (S), and focal distance (Z) to induce the production of visible graphitic structures. For that a 2 × 2 mm square matrix of P and S was done in each film to establish the range of values combinations could be used to produced LIG, **Figure 3**. Laser power used was around 4% and 5% of maximum operational value (2 W and 3 W, respectively), the speed scan in rast mode varied from 3% to 5% (38.1 mm/s and 63.5 mm/s) and focal distance was between 6 mm and 9 mm. As the films formulation and conformation were similar, no significant differences of laser parameters were needed since the underlying process of LIG formation is similar among all samples. It is important to note that it was possible to detect differences in the graphitic structure produced for different laser parameters. As expected, larger power values led to the complete ablation of films while low power values did not change the film's structure [46]. Additionally, it was possible to confirm that the scan speed also influences the production of graphitic layers as for a fixed P low scan speed led to

damaged films, as the substrate is submitted to high temperatures for higher periods of time per point, forming a melting-like structure instead of powder solid graphitic layer. Here we prove that it is possible to produce LIG in polysaccharide-based films with a single laser step, which was never been made to the best of our knowledge.

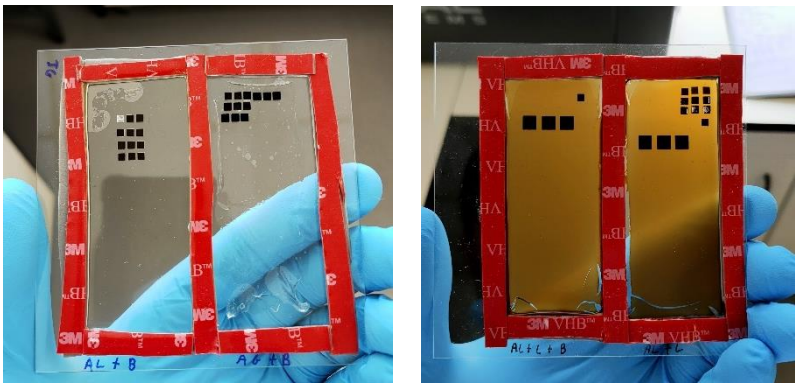

Figure 3. Images of the matrix of graphitization achieved in: alginate/borax, agarose/borax, alginate/borax/lignin, and alginate/lignin films, respectivitely.

3.3 LIG Characterization

This section presents the results of Raman spectroscopy and electrical conductivity studies, performed to evaluate the chemical and electrical properties of LIG produced in the different polysaccharide films. With this first analysis it was possible to select the best films formulations to produce LIG and thus the ones with suitable properties for cell experiments, based on their Raman spectra and sheet resistance values.

3.3.1 Raman Spectroscopy

Raman spectroscopy provides a fast, non-destructive molecular-level analysis that can be used to prove and evaluate the presence of graphene after laser scribing on a sample. This technique measures the polarization of molecules in the sample, by comparing stokes shifts, which are characteristic of different molecules [21]. The Raman spectra of multilayer graphene and graphite exhibit a simple structure composed of three principal bands, namely D, G and 2D bands [47]. The G band usually appears around 1580 cm^{-1} and represents the sp^2 hybridized carbon atoms present in the graphitic material. The D band, around 1350 cm^{-1}, known as the defect band, assesses the defects present in the sample. The 2D band, around 2700 cm^{-1}, is known as the second order of the D band, and is the result of the phonon lattice vibrational process [47]. As referred before, the first analysis focused on the comparison of Raman spectra of films within the same group, to evaluate the presence and efficiency of LIG produced in the different materials, through the study of the morphology of the three main peaks of graphene spectra. Visible graphitization occurred in all samples, however due to the high fluorescence of polysaccharide

films, Raman spectra of some samples were not successfully achieved. **Figure 4** shows the Raman data of LIG produced in the different films.

For the chitosan-based films data presented in **Figure 4 a)**, it is possible to see that the Raman spectra of LIG produced in chitosan and chitosan/lignin films doesn't show a significant D peak, indicating the poor quality of LIG in these samples. For the chitosan/borax and chitosan/borax/lignin samples, the corresponding spectra showed three predominant Raman peaks, confirming the presence of LIG. For agarose group, **Figure 4 b)**, it was not possible to obtain the spectra of LIG produced in agarose-only film, due to its high fluorescence. The other agarose containing films showed sharp D, G, and 2D peaks, being the agarose/borax/lignin the one that seems to have LIG with higher quality (defined by the ratios presented in 3.4.3). The Raman spectra of alginate group, **Figure 4 c)**, exhibit a significant 2D peak, and a broad D and G peaks, characteristic of amorphous carbon. For the three groups, a relationship between the presence of borax and/or lignin in the films and the graphene quality is perceptible. This result is expected, as these components are carbon precursors, contributing with aromatic content, which promotes the formation of graphitic structures.

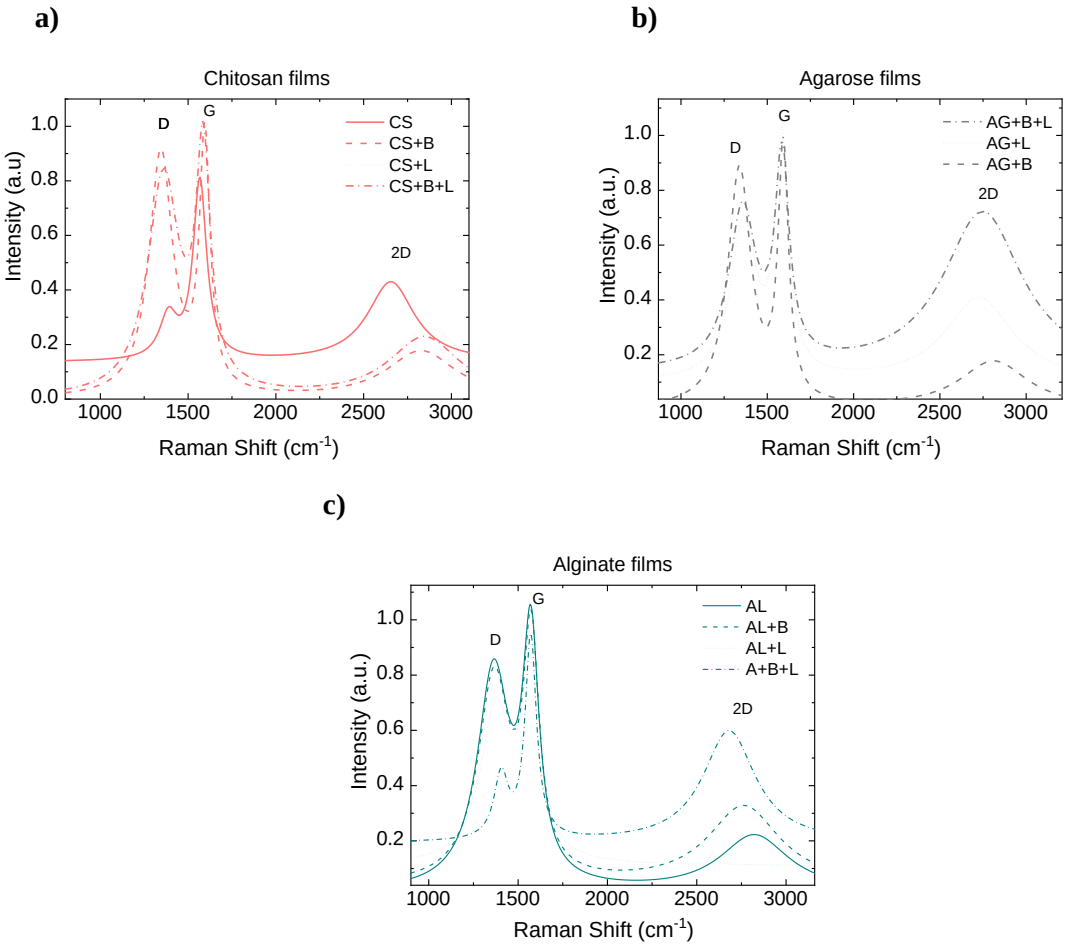

Figure 4. Raman spectra of LIG produced in the different groups of materials, with its characteristic D, G, and 2D peaks, respectively: **a)** chitosan films group, **b)** Agarose films group, **c)** Alginate films group.

It is important to mention that different films modifications, with different percentages of materials used, may enhance LIG formation. For instance, in Sinha et al.' study, it was proved that higher percentages of lignin in PDMS films, lead to the production of highly efficient LIG [21]. Moreover, a more thorough optimization of laser scribing parameters should allow the production of highly efficient LIG for all films, as it has already been proved that different laser speed and power lead to different types of graphitic structures [21], [29], [46].

3.3.2 Electrical Conductivity

The electrical conductivity analysis was performed in all samples, to evaluate the resistivity of the LIG produced in each film. These results were then crossed with the ones obtained with Raman to better understand the underlying LIG formation process. According to the hypothesis of this thesis, films with high quality LIG should show lower sheet resistance values, as their conductivity is improved by the presence of the graphitic layer.

A comparative analysis of the sheet resistance of the LIG produced in the different film formulations, **Figure 5**, shows that the graphitic layer improved the electrical conductivity of the polysaccharide films. Sheet resistance value of chitosan and agarose films was lower than that of the alginate films group. This is in accordance with the Raman spectroscopy analysis that showed LIG produced in alginate films was lower quality graphene, indicating the presence of a disorder structure instead of a crystalline structure of a high quality one. The presence of defects and disorder in low-quality graphene can lead to reduced electrical conductivity since electrical transport properties are disrupted. As expected, for all groups the R_{sheet} values of the polysaccharide-only films is higher than the modified films, showing an improvement in the conductivity with the presence of borax and/or lignin. Additionally, the presence of both borax and lignin showed an improvement in the sheet resistance in all films, indicating that this formulation allows the higher conductivity of the biopolymer's films. Nevertheless, these results were significantly higher than LIG from polyimide films (R_{sheet}< 50 Ω/sq) [26]. Polyimide has aromatic rings in its structure which provides a foundation for graphitization, as these rings can readily undergo carbonization and structural rearrangements to achieve a more graphitic structure. The polysaccharide materials are essentially composed by carbohydrates, which limit their graphitic potential and may require more extensive chemical or thermal modifications to achieve a similar degree of graphitization. Besides this, polyimide exhibits higher thermal stability, comparing to polysaccharide materials, allowing it to withstand the elevated temperatures required for graphitization processes. Additionally, another factor that can explain the lower sheet resistance values of the produced films may be related to the fact that polysaccharides often present more complex and irregular structures compared to the planar, aromatic structures found in polyimides. These structural complexities can present difficulties to achieving a highly ordered, graphitic structure.

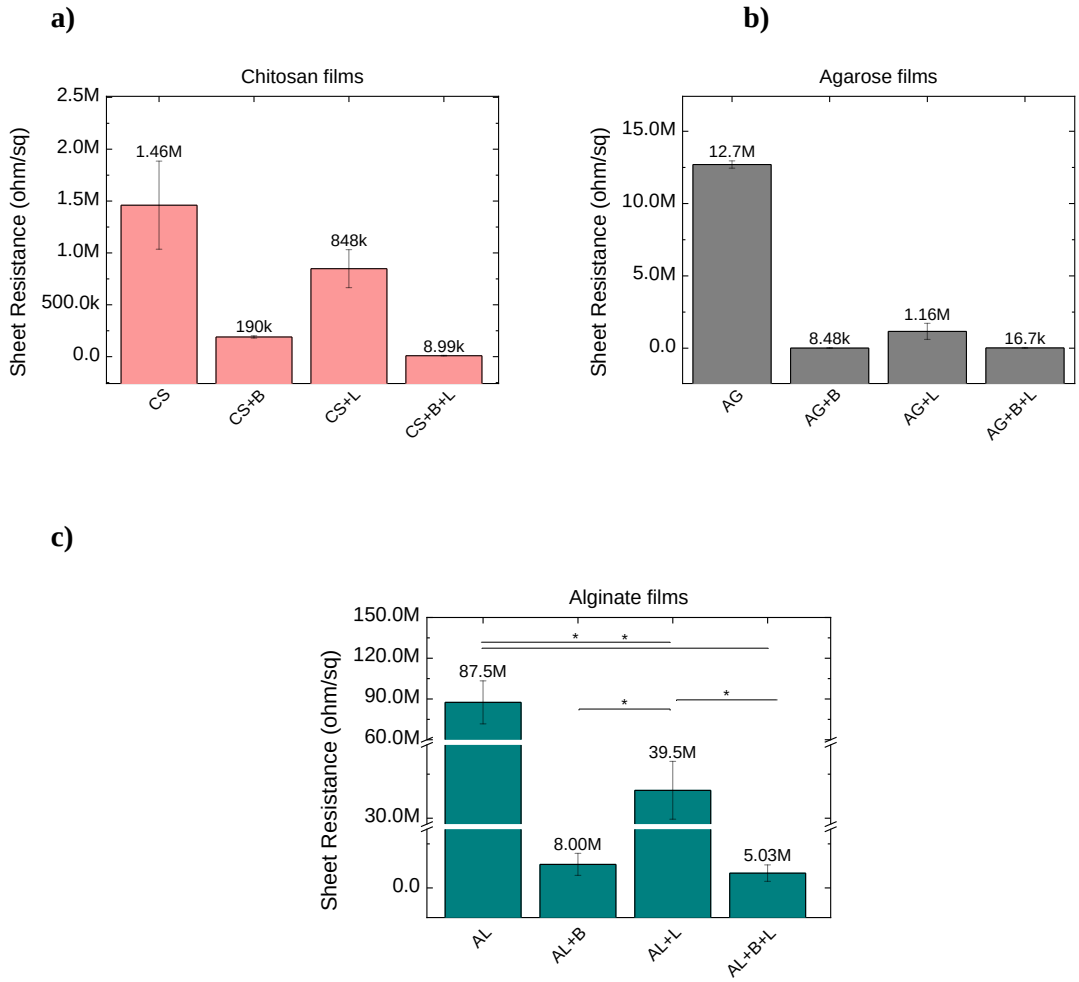

Figure 5. Sheet resistance data of the different film formulations after laser irradiation. **a)** chitosan films, **b)** agarose films, **c)** alginate films. Error bars present standard deviation (n=3). * when $p<0.05$ indicating only significant differences between samples within the alginate group.

These results suggest that further reductions in sheet resistance may be possible by optimizing the laser patterning process to enable the formation of 2D conduction paths. In Larrigy et al.' study they proved that 3 step laser process, with different laser wavelengths, improved the sheet resistance values of chitosan films, so another option may be increasing the number of laser steps, producing a more solid graphene layer. Another possible approach to achieve lower R_{sheet} values may be producing thinner and more uniform films, using the doctor-blade technique [29].

3.4 Best performing films

This section presents a detailed analysis of the morphological, mechanical, chemical, and electrical properties of three samples, which seem to be the appropriate for the experiments with cells based on Raman and electrical characterization results. The samples that seemed to have adequate chemical and electrical properties for our hypothesis were AGB, AGBL, and CSBL, as they showed the characteristic peaks in Raman spectra, and presented the lowest R_{sheet} values. Therefore agarose/borax film

(AGB), agarose/borax/lignin film (AGBL), and chitosan/borax/lignin film (CSBL) samples will be further study to ensure their viability as matrix to cell culture experiment, **Figure 6**.

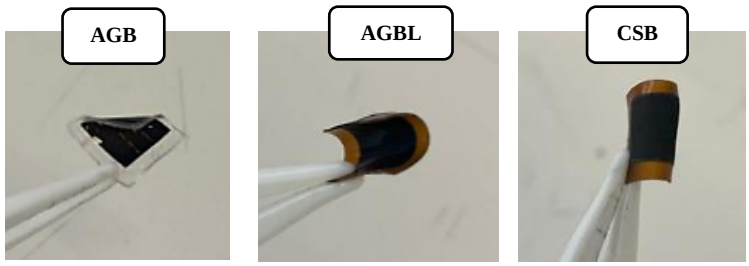

Figure 6. Photo of samples of the three films analyzed in this chapter: agarose/borax film (AGB), agarose/borax/lignin film (AGBL), and chitosan/borax/lignin film (CSBL, respectivetly) after immersion in cell culture medium for 15 days.

This analysis is composed of an evaluation of their swelling and degradation behavior in PBS solution, followed by morphology study using SEM. Additionally, Raman spectra of each sample is analyzed where peak intensities are compared to ascertain about LIG quality. Finally, the electrical conductivity analysis of samples is made by study of the sheet resistance and LIG thickness, which is measured through cross-sectional SEM images.

3.4.1 Swelling degree and degradation ratio

Moderate swelling degree and controlled degradation of scaffolds are desired for cell culture experiments, as they allow for a balance between retaining sufficient liquid for maintaining a stable environment and providing a precise control over culture conditions. Regarding swelling behavior, the three samples showed SD values after 48 h between 100 % and 600 %, remaining stable after the first 24 hours, **Figure 7 a)**. The stability of the films is essential to ensure a viable matrix along all the experiments with cells. Chitosan film, CSBL, showed a more linear behavior during the test, while agarose films, AGBL, and AGB, showed a higher increase in SD in the first 30 min of the experiment. This can be explained as agarose, contrarily to chitosan, is a water-soluble polymer, containing high number of hydrophilic groups (-OH) and high amorphous content [48]. As said above, the addition of borax in the formulation of the films may lead to a higher absorption ability, while the presence of lignin lead to a lower swelling behavior. In accordance, the sample AGB showed the highest SD value, while the two samples with lignin, AGBL, and CSBL, showed lower values, **Figure 7 a)**. Regarding degradation test, **Figure 7 b)**, the films had similar performance.

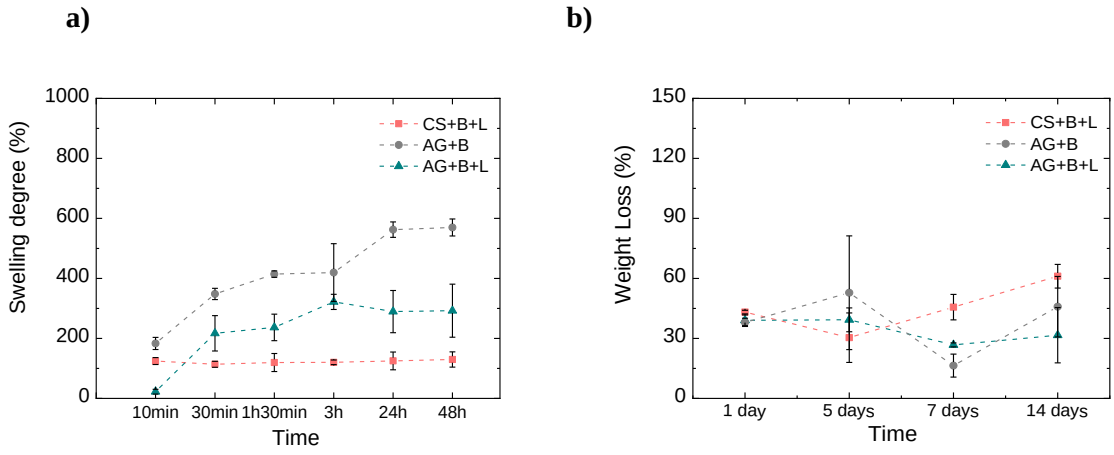

Figure 7. a) Swelling degree data of agarose/borax film (AGB), agarose/borax/lignin film (AGBL), and chitosan/borax/lignin film (CSBL) samples as function of immersion time in PBS solution (pH 7.4, RT). Data are shown as % increase in the film weight, as means ± SD (n=3 per group and time point). $p<0.05$ showing significant differences between AGB and CSBL groups **b)** Weight loss data of agarose/borax film (AGB), agarose/borax/lignin film (AGBL), and chitosan/borax/lignin film (CSBL) samples as function of immersion time in PBS solution (pH 7.4, 37 ºC). Data are shown as % difference in the film weight over the time, as means ± SD (n=3 per group and time point. $p>0.05$ indicating no significant differences between groups. Error bars represent standard deviations. $p>0.05$ showing no significant differences between groups.

3.4.2 Scanning electron microscopy (SEM) of LIG

The results of the surface morphology studies of LIG produced in the different samples are presented in **Figure 8**. It is shown that the formed LIG layer exhibits the appearance of a foam with porous structures resulting from the rapid libertation of gaseous products during laser scribing [26]. These porous structures render enhanced-accessible surface areas and facilitate liquid penetration into the active materials [26]. The porosity of graphene surface was assessed using ImageJ software, as well as pore size, (**Table 3**), showing a pore size < 4 µm. Since laser irradiation is a photothermal process, laser power is a crucial variable for inducing graphene from carbon precursors, resulting in different porosities and layered structures [49]. Higher laser power leads to a higher degree of graphitization, and consequently higher porosity [26]. Additionally, higher laser speed leads to larger pore sizes and higher porosity structures, due to shorter heat accumulation time [21]. LIG with larger porosity usually suggests poor electrical conductivity, once it has damaged electron conduction pathways compared with lower porosity, where LIG layers are close together. AGBL sample showed high porosity with high pore size when compared with AGB and CSBL, indicating that AGBL may present poorer electrical conductivity. However, LIG thickness also influence its electrical properties, so it needs to be considered.

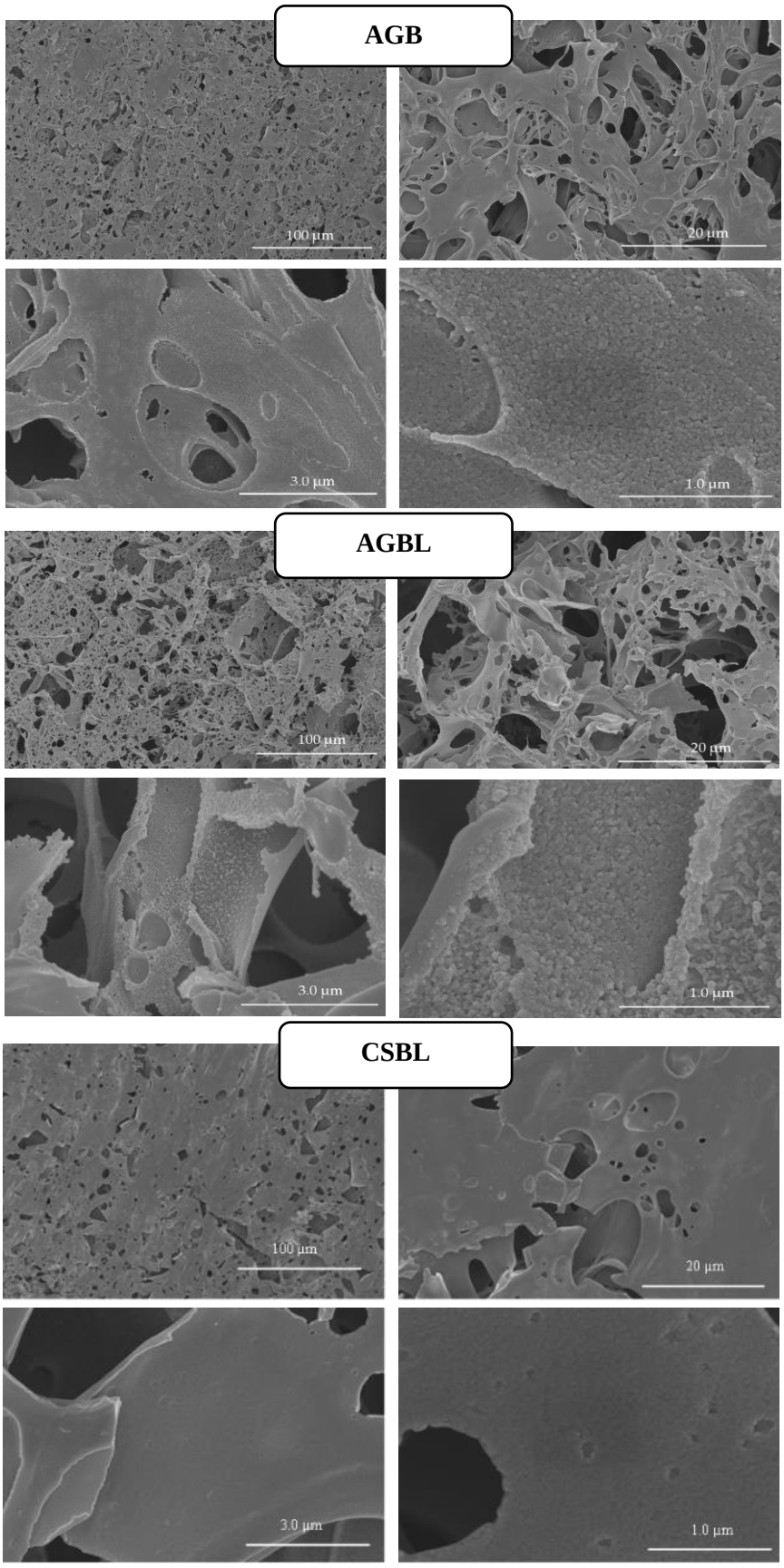

Figure 8. Scanning electron microscopy study of surface morphology of samples after laser scribing: agarose/borax film (AGB), agarose/borax/lignin film (AGBL), and chitosan/borax/lignin film (CSBL), respectively. Scale bars represent 100 µm, 20 µm, 3 µm, and 1 µm, respectively.

Table 3. Porosity data of samples, estimated with ImageJ software.

Sample	Porosity (%)	Average pore size (µm)
AGB	14.47 ± 2.98	1.39 ± 0.14
CSBL	15.75 ± 2.62	2.85 ± 1.32
AGBL	38.87 ± 7.19	3.13 ± 0.29

Results presented as mean ± SD (n=3).

Besides, the quality of graphene can also be assessed by studying the graphene layers. Cross-sectional SEM images of mechanically cleaved samples, **Figure 9** reveal 3D microporous LIG films with mean thickness values between 35 and 60 µm. Through the analysis of cross-section images of LIG, it was possible to measure thickness using ImageJ software. The results (**Table 6**) showed that LIG produced in AGBL sample presented the lowest thickness (37 µm), which was expected since its high porosity led to a smaller number of stable layers formed. Besides, thickness of LIG also influences its quality as higher thickness leads to higher resistivity, according to equation (3).

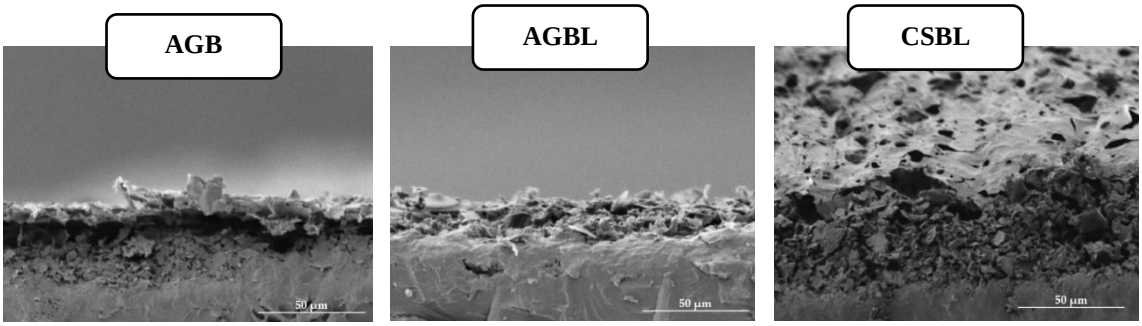

Figure 9. Scanning electron microscopy study of cross-sectional samples after laser scribing: agarose/borax film (AGB), agarose/borax/lignin film (AGBL), and chitosan/borax/lignin film (CSBL), respectively. Scale bars represent 50 µm.

3.4.3 Raman Spectroscopy

As mentioned previously in section 3.2.1,the Raman spectra of the three samples (AGB,AGBL,CSBL) show sharp peaks around 1350 cm^{-1}, 1580 cm^{-1}, and 2700 cm^{-1} (**Figure 10**) which can be ascribed as D, G, and 2D peaks and their detection confirms the presence of multilayer graphene.

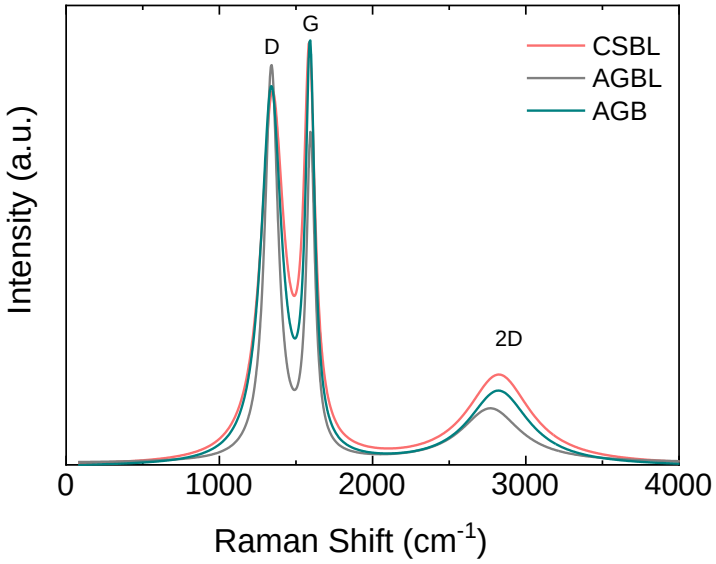

Figure 10. Raman spectra data of Lorentz fitting of the three samples, agarose/borax film (AGB), agarose/borax/lignin film (AGBL), and chitosan/borax/lignin film (CSBL), showing the characteristic D, G, and 2D peaks.

Besides the full width at half maximum (FWHM) of the 2D peak, the I_D/I_G and I_{2D}/I_G intensity ratios also give information about the efficiency of LIG production. FWHM analysis asses the number of layers in the graphitic structure, being higher for samples with a larger number of layers. The ratios also indicate the presence of multiple layers as well as the amount of disorder in LIG structure [22]. **Table 4** data shows FWHM values where CSBL and AGBL have the highest values, indicating the presence of multilayer LIG, while AGBL showed a more pristine LIG with less layers.

Table 4. Results for Lorentzian fits to Raman spectra.

Peak	**D**		**G**		**2D**	
Sample	**Pos (cm^{-1})** a)	**FWHM (cm^{-1})** b)	**Pos (cm^{-1})** a)	**FWHM (cm^{-1})** b)	**Pos (cm^{-1})** a)	**FWHM (cm^{-1})** b)
AG+B+L	1340±0.39	105±1.16	1596±0.38	67±1.12	2770±5.39	470±18.4
CS+B+L	1346±0.87	183±2.87	1587±0.55	88±1.77	2825±5.02	504±17.5
AG+B	1339±0.6	162±1.9	1592±0.36	72±1.16	2822±4.65	484±16

a) Pos: Peak Centre; b) FWHM: Full width at half-maximum intensity. Fit results presented as value ± standard error.

The peak intensity and area ratios were also analyzed to evaluate the quality of LIG produced in the different film formulations, **Figure 11**. Firstly, I_D/I_G ratio indicates the crystallite size of the graphitic carbon, with a negative correlation. Note that a high I_D/I_G ratio indicates low crystallite size [50]. Additionally, a high I_{2D}/I_G ratio indicates the number of defects present in the sample. Low I_{2D}/I_G ratio indicates multilayer graphene, high porosity, and high number of defects, which means that the samples

look like graphite instead of a single layer graphene (I_{2D}/I_G=2). The results showed that all samples presented lower I_{2D}/I_G ratio than single layer graphene, indicating that the graphitic structure formed was similar graphite. Besides, although the results are similar between the samples, it is possible to see some differences. CSBL sample showed the lowest I_D/I_G ratio (0.88), meaning that LIG formed in this sample is a more pristine and less defect. The opposite behavior was observed for the I_{2D}/I_G ratio, where CSBL showed the highest value at 0.21. This is an indicator that the LIG produced in CSBL sample has fewer layers than the one produced in AGBL and AGBL samples. The same analysis can be done with area under peaks results. AGB showed a very similar results, indicating that CSBL and AGB should be the samples with highly efficient LIG produced in this work. Additionally, Raman maps of the ratios corresponding to the several samples also show the difference among the samples, **Figure 11** where green color represents I_{2D}/I_G peak ratio while red color represents I_D/I_G peak ratio. It confirms that CSBL presents higher I_{2D}/I_G peak ratio and lowest I_D/I_G peak ratio, proving the presence of less defect dense graphitic material [47].

Table 5. Raman peak ratios data of the Lorentz fitting.

Ratio	Intensity		Area	
Sample	**I_D/I_G**	**I_{2D}/I_G**	**A_D/A_G**	**A_{2D}/A_G**
AG+B+L	1.20	0.16	0.86	1.86
CS+B+L	0.88	0.21	1.44	0.99
AG+B	0.89	0.18	0.82	1.82

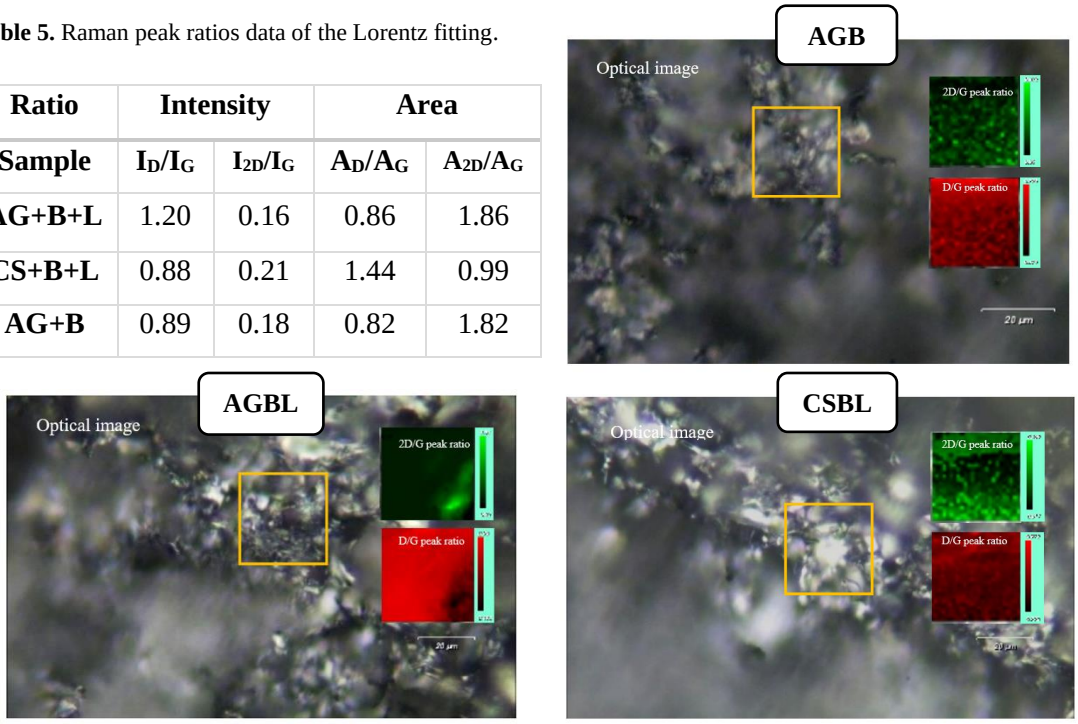

Figure 11. Table 5 of the Raman peak ratios data of the Lorentz fitting of the LIG produced in the three samples, showing the results of intensity peak ratio and area peak ratio. Raman peak ratio maps showing the distribution of the peak intensity along the selected area of the samples: agarose/borax film (AGB), agarose/borax/lignin (AGBL), and chitosan/borax/lignin film (CSBL). The green color represents I_{2D}/I_G peak ratio while red color represents I_D/I_G peak ratio.

3.4.4 Electrical Conductivity

An estimation of the conductivity of the LIG formed in the three samples, can be determined by combining the LIG thickness measured by cross-sectional SEM and the measured sheet resistance, **Table 6**.

Comparing the values, despite their similarity, the resistivity of LIG produced in CSBL is lower than agarose films, which is in accordance with the previous analysis. Once more, AGB presented similar results to CSBL. The combination of the lower R_{sheet} value, and low thickness of LIG produced in CSBL sample, make it the one with higher conductivity. However, as mentioned in section 3.3.2 these resistivity values are significantly higher than those of LIG fabricated from polyimide ($\rho = 8 \times 10^{-4}\ \Omega.m$) which may be related to the increased disorder in the polysaccharide films LIG, proved by the increased FWHM of the 2D peak versus polyimide LIG. This was expected, as these feedstock materials are highly variable in comparison to polyimide [30].

Table 6. Sheet resistance, LIG thickness and equivalent resistivity values.

Sample	**Sheet Resistance,** R_{sheet} (Ω/sq)	**LIG thickness**, t_{LIG} (µm)	**Resistivity,** ρ (Ω.m)	**Conductivity,** 1/ρ (S.m)
CSBL	8990 ± 119	50 ± 6	0.450	2.22
AGB	8480 ± 1327	59 ± 27	0.500	2
AGBL	16700 ± 100	37 ± 16	0.616	1.62

Results presented as mean ± standard error.

To electrically stimulate cells, it is essential to assure the ideal conductivity of the matrix to promote electrical signal propagation between cells and, consequently improve their metabolism and maturation. This because higher conductivity may damage cells, while low conductivity is not enough to stimulate the interactions between cells. Usually, conductivity values in the same order of magnitude as the ones of ventricular muscle, blood, and skeletal muscle ($0.03 - 0.6$ S/m) are necessary to guarantee a good compatibility between CM activity and the functionalized biopolymers [51] Although the obtained conductivity of LIG ($\approx 2\ S.m$) produced in this work may be low to some electronic applications, seem to be adequate to experiments with cells, which is the goal of this thesis. It is important to note that for use of these films in electrical stimulation of CM, it is required an adjustment in their conductivity to ensure the viability of cells.

3.5 Cell Culture Experiments

This section presents the results of the cell experiments done in this work, as well as their discussion. As said above, this thesis aims to exhibit the functionality of the films produced to be employed for electrical stimulation of cardiomyocytes in the future. Thus, we hypothesized that porous, electrically conductive polysaccharide substrates would improve cardiomyocyte activity and metabolism, which was proved with chitosan/carbon nanofibers scaffolds, even without electrical stimulation [52].

Since the previous analysis showed that LIG produced in AGB, AGBL, and AGB films has the appropriate electrical properties, presents sharp D, G, and 2D Raman peaks and showed good stability to contain cells for 14 days, these three samples were selected to be used with iPSC-CMs. Therefore, in this section, the samples analyzed are the AGB, AGBL, and CSBL, which will be used for the electrical stimulation tests afterwards. The goal here is to understand the effect of LIG in cell viability and function once it was never tested before according to our knowledge.

3.5.1 Cell Viability (Live/Dead assay)

The viability of LIG produced in the AGB, AGBL, and CSBL samples was assessed, firstly, by Live/Dead staining on different periods of time: 8 hours, 3 days, and 5 days. The viability of cells is influenced essentially by their ability to adhere to the biopolymer surface. Cell adhesion consists in the absorption of proteins from the culture medium onto the biopolymer surface, followed by the release of compounds from cells, ECM deposition, cell proliferation and lastly differentiation. All of these steps are influenced by the physical and chemical interaction of the cell and the substrate [53]. Chemical features of a substrate include surface charges, wettability, and protein adsorption ability, while physical properties include topography, and stiffness [53]. It is known that a rough surface improves cell adhesion in comparison with smooth surfaces [54]. Pore size also influences cell adhesion, as higher pore size affect cell seeding and migration (>8 μm), and nanopores may hamper the spread of nutrients and damage the functions of cells [54]. Additionality, cells are more likely to adhere to hydrophilic surfaces, with high wettability as these surfaces promote cell attachment. Regarding the influence of chemical properties of the substrate on cell adhesion, it has been proven that cells adhere better to positively charged surfaces than negatively charged ones [54]. The substrate formulation also affects cell adhesion as some components may be added to enhance biocompatibility and bioactivity, thus promoting cell attachment.

As shown in **Figure 12**, the viability of cells was different between the samples, showing a very constant behavior for AGBL and CSBL samples, while AGB showed a more variable behavior. This indicates that, throughout the cell culture time the number of live cells in AGBL and CSBL remained the same, while in AGB sample the number of cells varied during the different time points, increasing their number at day 5. Agarose film incorporated with borax (AGB) showed the highest number of live cells during the experiment, presenting a decrease on day 3, probably due to poor adhesion of cells in a early stage of the experiment. At the last time point of the experiment, day 5, cells cultured in AGB and CSBL showed high viability, as the area of live cells was higher, compared with the cells cultured in AGBL sample. Live cells appeared to be present in all the different samples and the different time points, indicating that the functionalized films were a stable environment for cell viability, especially for AGB and CSBL which seemed to be a more favorable environment for cells.

a)

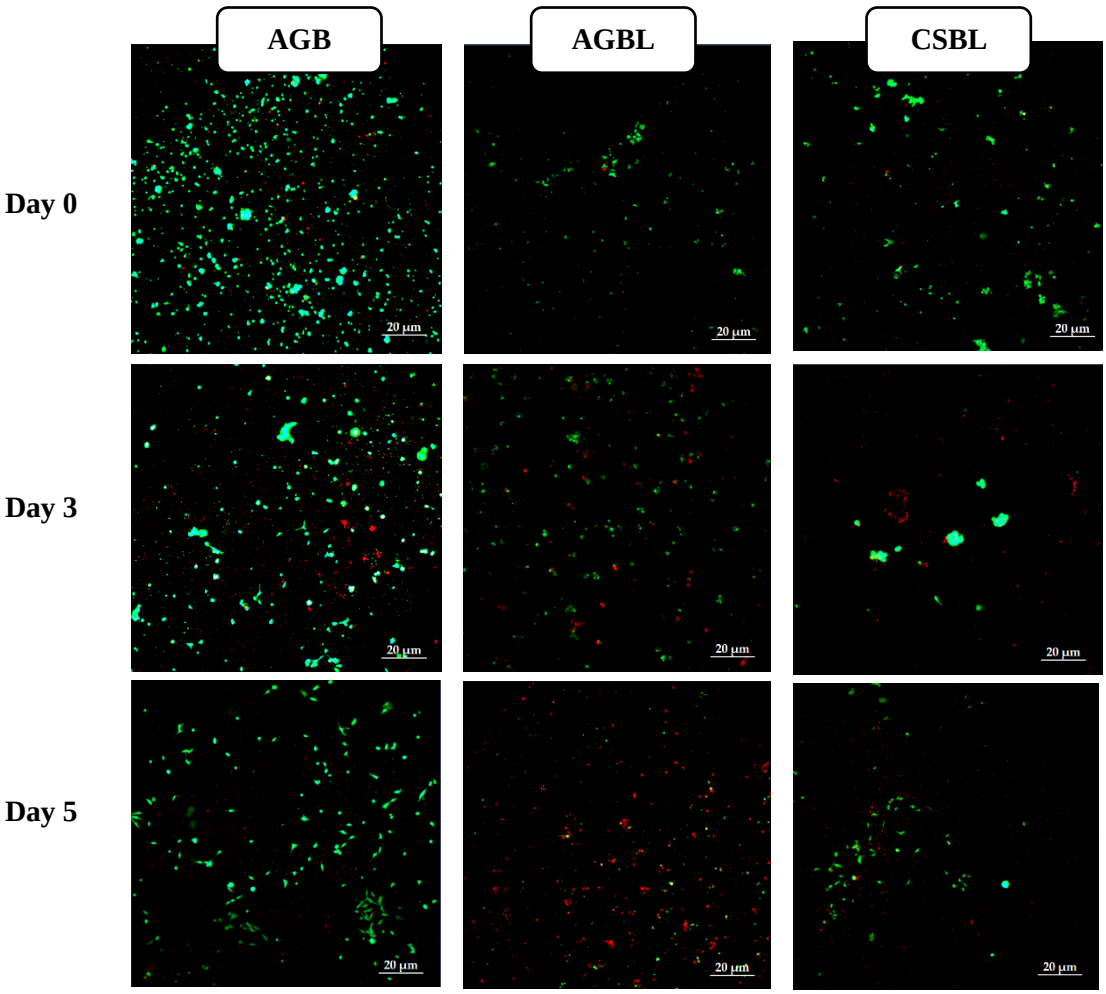

b)

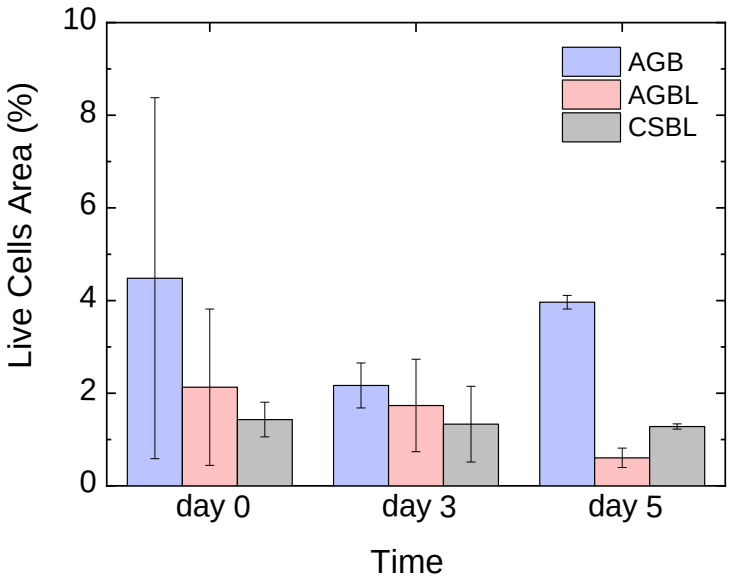

Figure 12. a) Representative image of live/dead assay for the LIG produced in agarose/borax film (AGB), agarose/borax/lignin film (AGBL), and chitosan/borax/lignin film (CSBL) throughout culture time by fluorescence microscopy, stained with fluorescein diacetate (FDA-live cells, green) and propidium iodide (PI-dead cells, red); Scale bars represent 20 µm **b)** Cell viability

data obtained using FIJI In ImageJ software, on 3 different timepoints (n= 3). Scale bars represent standard deviation. p>0.05 indicating no significant different between groups.

A qualitative analysis was also made of the cultured cells on day 5, **Figure 13**, where the cell morphology of the three samples is shown. As seen before, AGBL showed a lower number of live cells, which presented a rounded shaped while AGB and CSBL samples showed a larger number of elongated cells. This indicates that AGB and CSBL samples the adhesion of cells to the biopolymer was more efficient than in AGBL sample. In this work, the results showed that AGB and CSBL presented higher cell viability at day 5. This can be explained by the fact that these samples, presented the more adequate pore size and porosity of LIG. Additionally, as electrically conductive scaffolds improve cell function, samples with higher conductivity should have higher cell viability than lower conductive ones. Our results are in accordance with this hypothesis, as the AGB and CSBL samples showed higher conductivity and also higher cell viability.

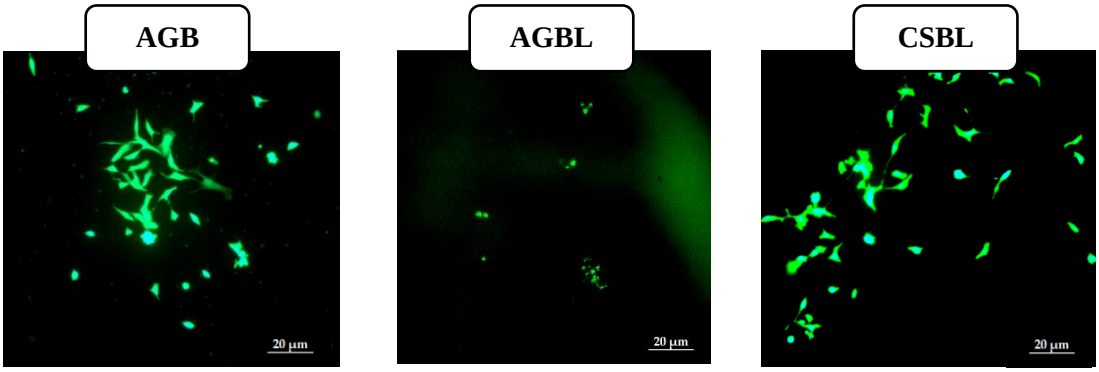

Figure 13. Image of live cells on day 5 of the Live/Dead experiment for agarose/borax film (AGB), agarose/borax/lignin film (AGBL), and chitosan/borax/lignin film (CSBL), respectively. Scale bars represent 20 µm.

3.5.2 Cell Metabolism (Presto Blue Assay)

Fluorescence analysis was performed to examine the impact of the biopolymers and LIG on cell proliferation throughout the cell culture time, **Figure 14**. The results showed a significant increase in the cell proliferation with the presence of the biopolymers, when compared with control group. Cells cultured in chitosan film, CSBL, presented markedly and significantly higher metabolic activity than in agarose films, AGBL and AGB. On the last day of the experiment, the cells cultivated in AGBL film showed a decrease in metabolic activity, which is in accordance with the results of Live/Dead analysis, where it was proved that AGBL sample was the one with less live cells at day 5 of cell culture. The fact that the CSBL showed higher metabolic activity may be related to the higher number of cells at the surface, while in agarose films cells seemed to be inside LIG. Importantly, cell viability was maintained throughout the duration of culture (5 days). Although these results suggest the non-toxicity of the functionalized polysaccharide films along the experiment, their behavior in a longer period of cell culture time should be evaluated.

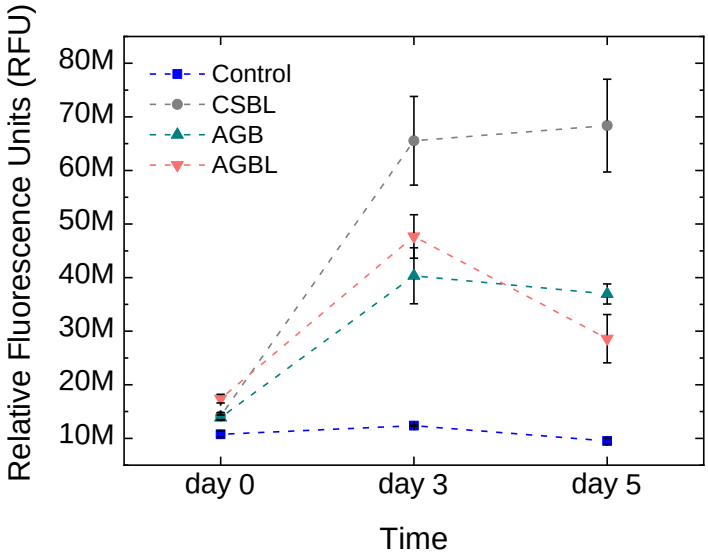

Figure 14. Graph of the results of Presto Blue assay of agarose/borax film (AGB), agarose/borax/lignin film (AGBL), chitosan/borax/lignin film (CSBL) and control group for 0, 3, and 5 days (n = 3 per sample and time point). Scale bars represent standard error. p>0.05 indicating no significant differences between groups.

3.5.3 Scanning Electron Microscopy (SEM) of cells

Morphological analysis by SEM, **Figure 15**, may be compromised as few cells were found in this analysis, which can be due to cells detachment from films during the ethanol baths. As so, the presented images may not be representative of cell distribution and morphology in all samples. Despite this, our results showed that at day 0, large amounts of extracellular matrix were secreted by cells in the AGB and CSBL samples, which is considered an essential factor for electrical signal conduction [55]. On the contrary, images of day 5 showed wide spreading cells and clusters, without extracellular matrix. Cells cultured in AGBL sample showed a more rounded shape and separated, while cells on CSBL films formed stable constructs, **Figure 15**. These results are in accordance with the previous analysis, indicating that agarose/borax film (AGB), and chitosan/borax/lignin film (CSBL) may offer a more favorable environment for cell adhesion and activity.

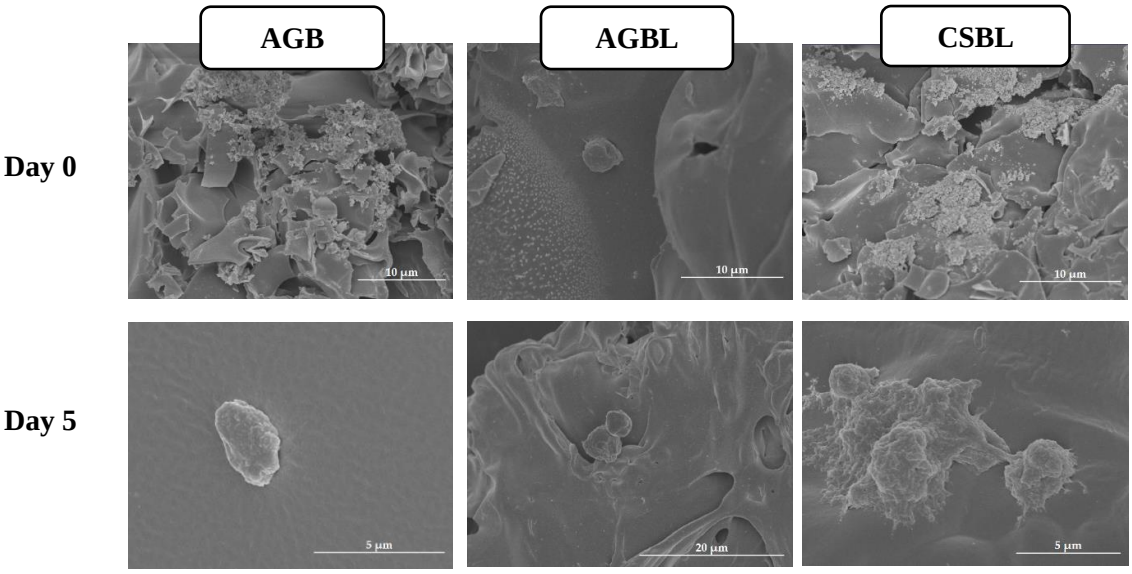

Figure 15. SEM images presenting the effect of LIG morphology in biopolymers at day 0 and day 5 of cell culture for agarose/borax film (AGB), agarose/borax/lignin film (AGBL), and chitosan/borax/lignin film (CSBL).

3.5.4 Immunofluorescence Staining

Due to high fluorescence of polysaccharide films, the immunofluorescent assay was compromised, and the results cannot be used for the analysis.

4. CONCLUSIONS

Recently, the need for sustainable and cost-effective solutions for cardiac tissue engineering have risen, seeking to innovate the cardiomyocytes (CMs) maturation to allow their use for therapeutic purpose. Laser-induced graphene (LIG) production process is nowadays considered a dominant technique employed to simultaneously produce and pattern graphene for several applications due to its cost-effectiveness and its suitability. Although the production of LIG from different substrates has been studied in the last decade, the use of natural, inexpensive, stretchable, and flexible is not yet completely comprehended, especially for their use in biomedical applications.

The goal of this thesis was to develop nature-derived conductive films for therapeutic applications for cell culture experiments, with a vision of improving cardiomyocyte maturation approaches used nowadays. Our approach hinged on the use of three marine-derived polysaccharides, namely chitosan, agarose, and alginate, to produce LIG to improve the electrical conductivity of the pristine films. Gathering the biocompatibility, and sustainability of the polysaccharide materials and the good electrical properties of graphene, our hypothesis was that these films would be an appropriate environment for cells, enhancing their metabolism and functionality.

Our research demonstrated that LIG can indeed be produced in polysaccharide films with a single laser step using a low-cost CO_2 laser, with optimized parameters. It was also proven that the incorporation of lignin and borax in the polysaccharide film formulation helped in the graphitization process, improving LIG quality. The results showed robust Raman peaks and reasonable sheet resistance values especially for the three detailed analyzed samples, agarose/borax film, agarose/borax/lignin film and chitosan/borax/lignin film confirming the quality of LIG produced.

In addition, the cell culture experiments using hiPSC-CMs have proven the biocompatibility of the polysaccharide films and the LIG produced in each one. Over 5 days of culture, we observed an improvement in cell metabolism and cell viability, especially for agarose/borax film, and chitosan/borax/lignin film. It was shown that the presence of low percentages of borax and lignin does not compromise cell viability and metabolism. Besides it was also proved that LIG porosity and morphology affect cell attachment, as higher porosity LIG showed fewer cells attached to the substrate. The LIG with a more robust structure, and higher conductivity showed higher cell viability, demonstrating that LIG may provide the required environment for cell signaling, adhesion and growth.

This pivotal discovery holds the promise for the application of these type of substrates for CMs maturation.

5. FUTURE WORK

Future studies should focus on testing various film formulations, with different percentages of polysaccharide material, borax, and lignin to evaluate the influence of each in the production of LIG. Concerning the laser scribing process, a more extensive optimization of laser parameters should be done to find the best combination for produce high quality LIG.

Additionality, further characterization of chemical and mechanical properties of polysaccharide substrates and corresponding LIG are required to ensure the efficiency of LIG production, namely UV/Vis absorption, X-Ray photoelectron spectroscopy (XPS), energy dispersive X-ray spectroscopy (EDS), Thermogravimetric Analysis (TGA), tensile strength (TS), percentage of elongation at break (ε), and Young's modulus (YM) [21]. Firstly, UV/Vis provides insights into the bandgap and energy levels of polysaccharide-LIG films, identifying any oxidized by-products from lasing process. XPS gives information about the elemental composition and chemical state of LIG's surface, indicating the percentage of material converted to graphene. EDS ensures the purity of LIG by making a depth analysis of chemical elements in the polysaccharide-LIG films. Regarding mechanical properties, TGA provides information about the film thermal stability, helping to determine the temperature range at which polysaccharide-LIG films remains stable. TS, ε, and YM asses the structural integrity and mechanical properties of LIG.

Cell experiments should be carried out during a longer culture time, the spontaneous beating and functionality of cardiac cells, as well as the mapping of the electrical signal transmission also should be evaluated, to understand the potential of these substrates for electrical stimulation of CM.

Overall, the use of conductive polysaccharide-LIG substrates can be the sustainable, low cost, and innovative solution for multiple therapeutic applications, as biosensing, bio electrochemical devices, and for tissue engineering. Additionality, polysaccharide-LIG substrates present also high potential for electronic application, such as miniaturized and wearable electronics, and sensors which has been gain a lot of interest in the last decade.

BIBLIOGRAPHY

[1] "Cardiovascular diseases." Accessed: Apr. 21, 2023. [Online]. Available: https://www.who.int/health-topics/cardiovascular-diseases#tab=tab_1

[2] O. Bergmann *et al.*, "Evidence for cardiomyocyte renewal in humans," *Science (1979)*, vol. 324, no. 5923, pp. 98–102, 2009, doi: 10.1126/science.1164680.

[3] "cardiac muscle | Definition, Function, & Structure | Britannica." Accessed: Oct. 23, 2022. [Online]. Available: https://www.britannica.com/science/cardiac-muscle

[4] Z. Lin and W. T. Pu, "Strategies for Cardiac Regeneration and Repair," *Sci Transl Med*, vol. 6, no. 239, p. 239rv1, Jun. 2014, doi: 10.1126/scitranslmed.3006681.

[5] Y. Guo and W. T. Pu, "Cardiomyocyte Maturation: New Phase in Development," *Circ Res*, vol. 126, no. 8, pp. 1086–1106, 2020, doi: 10.1161/CIRCRESAHA.119.315862.

[6] J. A. Roacho-Pérez *et al.*, "Artificial Scaffolds in Cardiac Tissue Engineering," *Life 2022, Vol. 12, Page 1117*, vol. 12, no. 8, p. 1117, Jul. 2022, doi: 10.3390/LIFE12081117.

[7] "Biodegradable polymers.pdf."

[8] J. Maughan *et al.*, "Collagen/pristine graphene as an electroconductive interface material for neuronal medical device applications," *Appl Mater Today*, vol. 29, no. July, p. 101629, Dec. 2022, doi: 10.1016/j.apmt.2022.101629.

[9] F. Zhang *et al.*, "Gelatin-based hydrogels combined with electrical stimulation to modulate neonatal rat cardiomyocyte beating and promote maturation," *Biodes Manuf*, vol. 4, no. 1, pp. 100–110, Mar. 2021, doi: 10.1007/S42242-020-00100-9.

[10] M. Soleimanpour, S. S. Mirhaji, and S. Jafari, "Designing a new alginate - fibrinogen biomaterial composite hydrogel for wound healing," pp. 1–17, 2022.

[11] C. B. Marín *et al.*, "Silk Polymers and Nanoparticles: A Powerful Combination for the Design of Versatile Biomaterials," *Front Chem*, vol. 8, no. December, pp. 1–22, Dec. 2020, doi: 10.3389/fchem.2020.604398.

[12] J. Sun and H. Tan, "Alginate-Based Biomaterials for Regenerative Medicine Applications," *Materials*, vol. 6, no. 4, p. 1285, 2013, doi: 10.3390/MA6041285.

[13] R. J. Hickey and A. E. Pelling, "Cellulose biomaterials for tissue engineering," *Front Bioeng Biotechnol*, vol. 7, no. MAR, pp. 1–15, Mar. 2019, doi: 10.3389/fbioe.2019.00045.

[14] I. A. Kadhim, Z. J. Abdul Ameer, and A. B. Alzubaidi, "Investigation of Chitosan Film Degradation in Tissue Engineering Applications," *IOP Conf Ser Mater Sci Eng*, vol. 671, no. 1, p. 012060, Jan. 2020, doi: 10.1088/1757-899X/671/1/012060.

[15] M. Boffito, S. Sartori, and G. Ciardelli, "Polymeric scaffolds for cardiac tissue engineering: requirements and fabrication technologies," *Polym Int*, vol. 63, no. 1, pp. 2–11, Jan. 2014, doi: 10.1002/PI.4608.

[16] L. Bačáková, K. Novotná, and M. Pařízek, "Polysaccharides as cell carriers for tissue engineering: The use of cellulose in vascular wall reconstruction," *Physiol Res*, vol. 63, no. SUPPL., 2014, doi: 10.33549/physiolres.932644.

[17] W. L. Stoppel, D. L. Kaplan, and L. D. Black, “Electrical and mechanical stimulation of cardiac cells and tissue constructs,” *Adv Drug Deliv Rev*, vol. 96, p. 135, Jan. 2016, doi: 10.1016/J.ADDR.2015.07.009.

[18] R. E. Ahmed, T. Anzai, N. Chanthra, and H. Uosaki, “A Brief Review of Current Maturation Methods for Human Induced Pluripotent Stem Cells-Derived Cardiomyocytes,” *Front Cell Dev Biol*, vol. 8, p. 178, Mar. 2020, doi: 10.3389/FCELL.2020.00178/BIBTEX.

[19] P. Machiraju and S. C. Greenway, “Current methods for the maturation of induced pluripotent stem cell-derived cardiomyocytes,” *World J Stem Cells*, vol. 11, no. 1, p. 33, Jan. 2019, doi: 10.4252/WJSC.V11.I1.33.

[20] V. V. Kodolova-Chukhontseva *et al.*, “Conducting Composite Material Based on Chitosan and Single-Wall Carbon Nanotubes for Cellular Technologies,” *Polymers 2022, Vol. 14, Page 3287*, vol. 14, no. 16, p. 3287, Aug. 2022, doi: 10.3390/POLYM14163287.

[21] K. Sinha, “Laser Induced Graphene on Lignin Upgraded Stretchable Polymer Films,” 2020, doi: 10.7939/R3-XB20-TA81.

[22] J. Maughan *et al.*, “Collagen/pristine graphene as an electroconductive interface material for neuronal medical device applications,” *Appl Mater Today*, vol. 29, p. 101629, Dec. 2022, doi: 10.1016/j.apmt.2022.101629.

[23] G. Ban, Y. Hou, Z. Shen, J. Jia, L. Chai, and C. Ma, “Potential Biomedical Limitations of Graphene Nanomaterials,” *Int J Nanomedicine*, vol. 18, p. 1695, 2023, doi: 10.2147/IJN.S402954.

[24] D. S. Bergsman, B. A. Getachew, C. B. Cooper, and J. C. Grossman, “Preserving nanoscale features in polymers during laser induced graphene formation using sequential infiltration synthesis,” *Nat Commun*, vol. 11, no. 1, pp. 1–8, Dec. 2020, doi: 10.1038/s41467-020-17259-5.

[25] B. Kulyk *et al.*, “Laser-Induced Graphene from Paper for Mechanical Sensing,” *ACS Appl Mater Interfaces*, vol. 13, no. 8, pp. 10210–10221, 2021, doi: 10.1021/acsami.0c20270.

[26] J. Lin *et al.*, “Laser-induced porous graphene films from commercial polymers,” *Nature Communications 2014 5:1*, vol. 5, no. 1, pp. 1–8, Dec. 2014, doi: 10.1038/ncomms6714.

[27] T. Pinheiro *et al.*, “Laser-Induced Graphene on Paper toward Efficient Fabrication of Flexible, Planar Electrodes for Electrochemical Sensing,” *Adv Mater Interfaces*, vol. 8, no. 22, pp. 1–12, Nov. 2021, doi: 10.1002/admi.202101502.

[28] R. Miyakoshi, S. Hayashi, M. Terakawa, R. Miyakoshi, S. Hayashi, and M. Terakawa, “Direct Patterning of Conductive Structures on Hydrogels by Laser-Based Graphitization for Supercapacitor Fabrication,” *Adv Electron Mater*, p. 2201277, 2023, doi: 10.1002/AELM.202201277.

[29] C. Larrigy *et al.*, “Porous 3D Graphene from Sustainable Materials: Laser Graphitization of Chitosan,” *Adv Mater Technol*, vol. 8, no. 4, p. 2201228, Feb. 2023, doi: 10.1002/ADMT.202201228.

[30] M. Katalinich, “Characterization of Chitosan Films for Cell Culture Applications,” pp. 1–196, 2001.

[31] P. Zarrintaj *et al.*, “Agarose-based biomaterials for tissue engineering,” *Carbohydr Polym*, vol. 187, pp. 66–84, May 2018, doi: 10.1016/J.CARBPOL.2018.01.060.

[32] Y. Lei, A. H. Alshareef, W. Zhao, and S. Inal, “from Lignin for Biochemical Sensing Laser-Scribed Graphene Electrodes Derived from Lignin for Biochemical Sensing,” *ACS Appl Nano Mater*, vol. 3, no. 2, pp. 1166–1174, Feb. 2019, doi: 10.1021/acsanm.9b01795.

[33] R. Miyakoshi, S. Hayashi, M. Terakawa, R. Miyakoshi, S. Hayashi, and M. Terakawa, “Direct Patterning of Conductive Structures on Hydrogels by Laser-Based Graphitization for Supercapacitor Fabrication,” *Adv Electron Mater*, p. 2201277, Mar. 2023, doi: 10.1002/AELM.202201277.

[34] J. A. Menima-Medzogo *et al.*, “Characterization and In Vitro Cytotoxicity Safety Screening of Fractionated Organosolv Lignin on Diverse Primary Human Cell Types Commonly Used in Tissue Engineering,” *Biology (Basel)*, vol. 11, no. 5, p. 696, May 2022, doi: 10.3390/BIOLOGY11050696/S1.

[35] M. N. A. M. Taib *et al.*, “Current progress of biopolymer-based flame retardant,” *Polym Degrad Stab*, vol. 205, p. 110153, Nov. 2022, doi: 10.1016/J.POLYMDEGRADSTAB.2022.110153.

[36] A. P. Franco-Bacca *et al.*, “Heat Transfer in Cassava Starch Biopolymers: Effect of the Addition of Borax,” *Polymers (Basel)*, vol. 13, no. 23, Dec. 2021, doi: 10.3390/POLYM13234106.

[37] “Scientific Opinion on the re-evaluation of boric acid (E 284) and sodium tetraborate (borax) (E 285) as food additives,” *EFSA Journal*, vol. 11, no. 10, Oct. 2013, doi: 10.2903/J.EFSA.2013.3407.

[38] J. M. Inácio, M. M. Nunes, M. Almeida, F. Cristo, R. Anjos, and J. A. Belo, “Gene-Edited Human-Induced Pluripotent Stem Cell Lines to Elucidate DAND5 Function throughout Cardiac Differentiation,” *Cells*, vol. 12, no. 4, p. 520, Feb. 2023, doi: 10.3390/CELLS12040520/S1.

[39] “LIVE/DEAD™ Viability/Cytotoxicity Kit, for mammalian cells.” Accessed: Jul. 26, 2023. [Online]. Available: https://www.thermofisher.com/order/catalog/product/L3224?SID=srch-srp-L3224

[40] J. Claus, A. Brietzke, C. Lehnert, S. Oschatz, N. Grabow, and U. Kragl, “Swelling characteristics and biocompatibility of ionic liquid based hydrogels for biomedical applications,” *PLoS One*, vol. 15, no. 4, Apr. 2020, doi: 10.1371/JOURNAL.PONE.0231421.

[41] B. Li, J. Wang, Q. Gui, and H. Yang, “Drug-loaded chitosan film prepared via facile solution casting and air-drying of plain water-based chitosan solution for ocular drug delivery,” *Bioact Mater*, vol. 5, no. 3, pp. 577–583, Sep. 2020, doi: 10.1016/J.BIOACTMAT.2020.04.013.

[42] M. A. Cerqueira, B. W. S. Souza, J. A. Teixeira, and A. A. Vicente, “Effect of glycerol and corn oil on physicochemical properties of polysaccharide films – A comparative study,” *Food Hydrocoll*, vol. 27, no. 1, pp. 175–184, May 2012, doi: 10.1016/J.FOODHYD.2011.07.007.

[43] Z. Ebadi, H. Ghaisari, B. Tajeddin, and S. S. Shekarforoush, “Production and evaluation of the chemical and mechanical properties of nanocellulose and nanowood starch-based biodegradable films potential candidates for moisture absorbers for food packaging,” *Food Sci Nutr*, vol. 9, no. 4, pp. 2227–2233, Apr. 2021, doi: 10.1002/FSN3.2194.

[44] S. Tanpichai, F. Phoothong, and A. Boonmahitthisud, “Superabsorbent cellulose-based hydrogels cross-liked with borax,” *Scientific Reports 2022 12:1*, vol. 12, no. 1, pp. 1–12, May 2022, doi: 10.1038/s41598-022-12688-2.

[45] M. Michelin, A. M. Marques, L. M. Pastrana, J. A. Teixeira, and M. A. Cerqueira, "Carboxymethyl cellulose-based films: Effect of organosolv lignin incorporation on physicochemical and antioxidant properties," *J Food Eng*, vol. 285, no. April, 2020, doi: 10.1016/j.jfoodeng.2020.110107.

[46] T. Pinheiro *et al.*, "Laser-Induced Graphene on Paper toward Efficient Fabrication of Flexible, Planar Electrodes for Electrochemical Sensing," *Adv Mater Interfaces*, vol. 8, no. 22, pp. 1–12, Nov. 2021, doi: 10.1002/admi.202101502.

[47] M. Wall, "The Raman Spectroscopy of Graphene and the Determination of Layer Thickness," *Thermo scientific*, p. 5, 2011.

[48] E. A. El-Hefian, M. M. Nasef, and A. H. Yahaya, "Preparation and characterization of chitosan/agar blended films: Part 2. Thermal, Mechanical, and surface properties," *E-Journal of Chemistry*, vol. 9, no. 2, pp. 510–516, 2012, doi: 10.1155/2012/285318.

[49] F. Mahmood, C. Zhang, Y. Xie, D. Stalla, J. Lin, and C. Wan, "Transforming lignin into porous graphene via direct laser writing for solid-state supercapacitors," *RSC Adv*, vol. 9, no. 39, pp. 22713–22720, 2019, doi: 10.1039/C9RA04073K.

[50] Y. Chyan, R. Ye, Y. Li, S. P. Singh, C. J. Arnusch, and J. M. Tour, "Laser-Induced Graphene by Multiple Lasing: Toward Electronics on Cloth, Paper, and Food," *ACS Nano*, vol. 12, no. 3, pp. 2176–2183, Mar. 2018, doi: 10.1021/acsnano.7b08539.

[51] A. M. Martins, G. Eng, S. G. Caridade, J. F. Mano, R. L. Reis, and G. Vunjak-Novakovic, "Electrically Conductive Chitosan/Carbon Scaffolds for Cardiac Tissue Engineering," *Biomacromolecules*, vol. 15, no. 2, p. 635, Feb. 2014, doi: 10.1021/BM401679Q.

[52] A. M. Martins, G. Eng, S. G. Caridade, J. F. Mano, R. L. Reis, and G. Vunjak-Novakovic, "Electrically conductive chitosan/carbon scaffolds for cardiac tissue engineering," *Biomacromolecules*, vol. 15, no. 2, pp. 635–643, Feb. 2014, doi: 10.1021/BM401679Q/ASSET/IMAGES/LARGE/BM-2013-01679Q_0007.JPEG.

[53] M. Ermis, E. Antmen, and V. Hasirci, "Micro and Nanofabrication methods to control cell-substrate interactions and cell behavior: A review from the tissue engineering perspective," *Bioact Mater*, vol. 3, no. 3, p. 355, Sep. 2018, doi: 10.1016/J.BIOACTMAT.2018.05.005.

[54] S. Cai, C. Wu, W. Yang, W. Liang, H. Yu, and L. Liu, "Recent advance in surface modification for regulating cell adhesion and behaviors," *Nanotechnol Rev*, vol. 9, no. 1, pp. 971–989, Jan. 2020, doi: 10.1515/NTREV-2020-0076/ASSET/GRAPHIC/J_NTREV-2020-0076_FIG_011.JPG.

[55] L. Jiang *et al.*, "Preparation of an Electrically Conductive Graphene Oxide/Chitosan Scaffold for Cardiac Tissue Engineering," *Appl Biochem Biotechnol*, vol. 188, no. 4, pp. 952–964, Aug. 2019, doi: 10.1007/S12010-019-02967-6.

APPENDIX

A.1 Mold used for the films fabrication

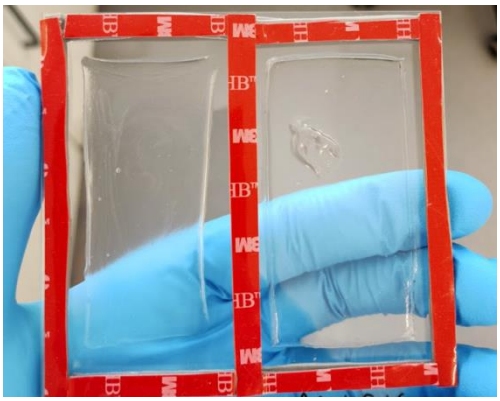

Figure 16. Example of the mould use for the fabrication of films using solvent casting method, at room temperature. The films illustrated in the photo are agarose film (AG) and agarose/borax film (AGB).

A.2 Films Conformation

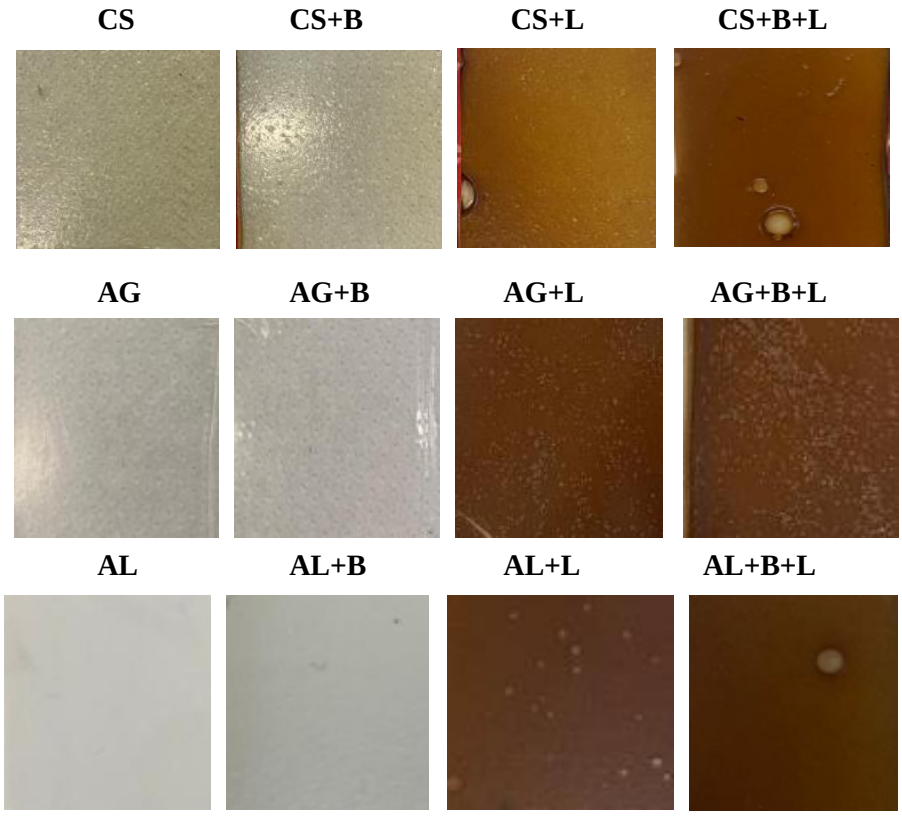

Figure 17. Photo of the differnt films, showing their conformation after fully dried.

A.3 Example of laser parameters matrix done in the films

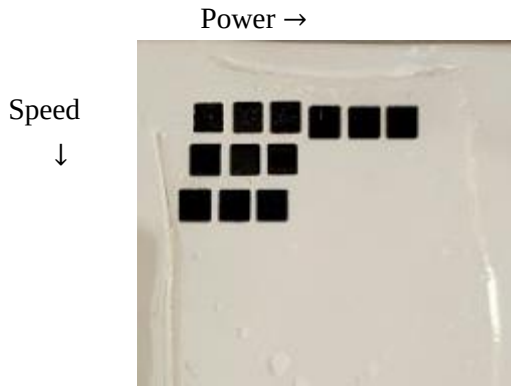

Figure 18. Photo of a matrix of laser parameters done in agarose/borax film, where are tested different laser power and speed.

A.4 Swelling degree curve

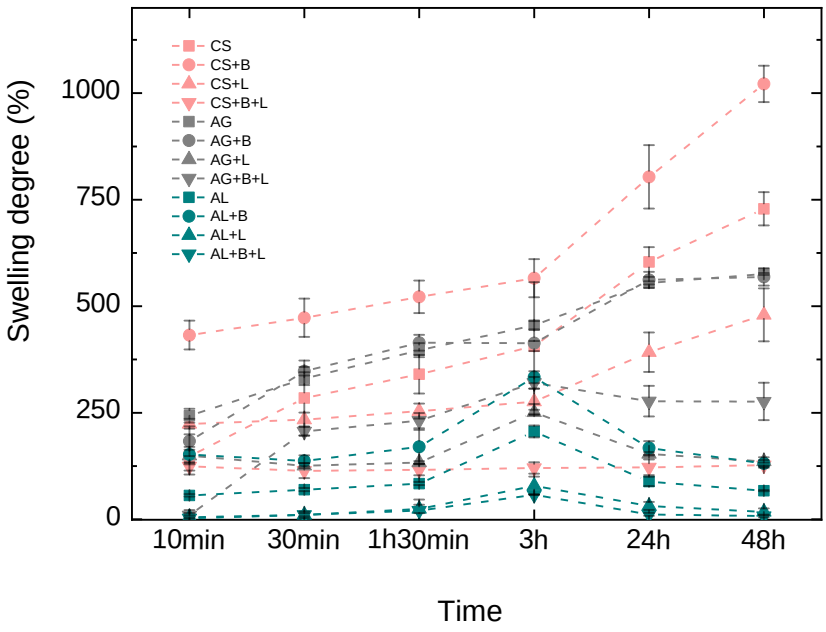

Figure 19. Swelling Degree data of the different film formulations, for different periods of time: 10 min, 30 min, 1h 30 min, 3 h, 24 h, and 48 h. Data are shown as % increase in the film weight, as means ± SD (n=3 per group and time point).

2023